ELECTRIC AND MAGNETIC DIPOLE FOR QUASI-OMNIDIRECTIONAL ULTRA HIGH FREQUENCY TAG DESIGN

LIM YI XIAN

A project report submitted in partial fulfilment of the requirements for the award of Bachelor of Engineering (Honours) Electronic and Communications Engineering

Lee Kong Chian Faculty of Engineering and Science
Universiti Tunku Abdul Rahman

JAN 2019

DECLARATION

I hereby declare that this project report is based on my original work except for citations and quotations which have been duly acknowledged. I also declare that it has not been previously and concurrently submitted for any other degree or award at UTAR or other institutions.

Signature : _____

Name : LIM YI XIAN

ID No. : 1403620

Date : 15/04/2019

APPROVAL FOR SUBMISSION

I certify that this project report entitled **"ELECTRIC AND MAGNETIC DIPOLE FOR QUASI-OMNIDIRECTIONAL UHF TAG DESIGN"** was prepared by **LIM YI XIAN** has met the required standard for submission in partial fulfilment of the requirements for the award of Bachelor of Engineering (Honours) Electronic and Communications Engineering at Universiti Tunku Abdul Rahman.

Approved by,

Signature	:	
Supervisor	:	PROF. IR. DR. CHUNG BOON KUAN
Date	:	15/04/2019

Signature	:	
Co-Supervisor	:	PROF. TS. DR LIM ENG HOCK
Date	:	15/04/2019

ACKNOWLEDGEMENTS

I would like to thank everyone who had contributed to the successful completion of this project. I would like to express my gratitude to my research supervisor, Prof. Ir. Dr. Chung Boon Kuan as well as my co-supervisor Prof. Ts. Dr. Lim Eng Hock for their invaluable advice, guidance and their enormous patience throughout the development of the research.

In addition, I would also like to express my gratitude to my loving parent, friends and seniors who had helped and given me encouragement throughout the whole project.

ELECTRIC AND MAGNETIC DIPOLE FOR QUASI-OMNIDIRECTIONAL ULTRA HIGH FREQUENCY TAG DESIGN

ABSTRACT

A compact tag antenna with a size of 45 mm x 45 mm x 3.379 mm (0.1374 λ x 0.1374 λ x 0.0103 λ) is proposed for a metal-mountable applications in the UHF RFID band. The compact tag antenna consists of two bowtie like dipoles. These dipoles are designed by using the concept of electric and magnetic dipoles. The first dipole (electric dipole) is aligned vertically onto the first foam while the second dipole (magnetic dipole) is aligned horizontally onto the second foam. This combination of dipole configuration enable the tag antenna to radiate in quasi-omnidirectional direction. The compact tag antenna is made up by three layers of metal patch which are electric dipole, magnetic dipole and ground. Conjugate match is achieved between the tag antenna and the Monza-5 chip. The realized gain of the tag antenna is 2.554 dB. The tag antenna has a readable distance of 13 m with EIRP power of 4 W. The resonant frequency of this tag antenna is 0.916 GHz which complies with the UHF RFID band. The power transmission coefficient of the tag antenna is 0.9047. The tag antenna is attached onto a 20 cm x 20 cm metal plate in the measurement process. The operating frequency is stable and insensitive to the changing of backing metal size.

TABLE OF CONTENTS

LIST OF TABLES

LIST OF FIGURES

LIST OF SYMBOLS / ABBREVIATIONS

S_{11}	reflection coefficient
S_{22}	reflection coefficient
S_{12}	reverse isolation
S_{21}	insertion loss
Γ_{in}	reflection coefficient at input port
Γ_{out}	reflection coefficient at output port
IL	insertion loss, dB
I_{rev}	reverse isolation, dB
ε_r	dielectric constant
f	frequency, Hz
λ	wavelength, m
c	speed of light, m/s
r_{tag}	read range of the tag antenna, m
P_t	transmitting power of the reader, W
P_{th}	sensitivity of tag, W
G_t	gain of the tag antenna, dB
G_r	gain of the reader, dB
τ	transmission coefficient,
d	length and width of the tag antenna, mm
l_1	half length of the top patch, mm
l_2	length of the slot for top patch, mm
l_3	length of the shorter side of middle bowtie patch, mm
l_4	length of the longer side of middle bowtie patch, mm
l_5	length of the stub, mm
W_1	width of the shorter side for middle patch, mm
W_2	width of top slot, mm
W_3	width between the slot, mm
W_4	width from slot to the end, mm
W_5	width of the bottom slot, mm
W_6	width of the stub, mm
t_1	thickness of foam, mm
g_1	gap of the chip, mm

V	Voltage, V
I	Current, A
L	Inductance, H
X_L	Inductive reactance, Ω

RFID	radio frequency identification
UHF	ultra high frequency
SNR	signal to noise ratio
PET	polyethylene terephthalate
CST MWS	CST Microwave Studio 2018
USD	United States Dollar

CHAPTER 1

INTRODUCTION

1.1 Background

Radio frequency identification (RFID) is a sort of rising innovation that utilize the electromagnetic field to recognize and read the labels that are attached on a specific object. A complete RFID system comprises two parts: a tag and a reader. RFID reader come with a transmitter and a receiver to transmit and receive data.

RFID tag is a little microchip attached to a small antenna to support wireless data transmission. It is usually attached to objects like a conventional glue sticker. The microchip size can be somewhere around 0.4 mm^2. A RFID tag transmits signals that contain information over the air in light of cross examination by a RFID reader.

RFID is an innovative technology for mechanized distinguishing proof of items and individuals. People are apt at recognizing objects under an assortment of test conditions. RFID can be used as a methods for labelling objects. For instance, every object in a warehouse is attached with a RFID tag containing the information of each object and this can help to reduce the workload of the worker. RFID tags are used as a part of numerous enterprises. For instance, a RFID tag is attached to an automobile during production phase in order to track the progress of the assembly line. Besides that, an embedded RFID microchips in the animals and pets are able to distinguish the proof or identification of the creatures.

According to some studies, the RFID global market was worth 8.89 billion USD in 2014. The RFID global market is expected to rise to 18.68 USD by 2026 **(Raghu, 2018)**. From these studies, I can foresee that the application of RFID technology is becoming an integral part in our daily life. Hence, I had chosen RFID technology as my final year project.

1.2 Problem Statement

In this modern era, technologies are keep on improving. One of these technologies is RFID technology. RFID technology is a rising technology that utilizes the electromagnetic field to recognize and read the labels of the RFID tag. RFID technology is becoming an integral part in our daily live. However, designing a RFID tag is a very difficult task since the RFID technology is keep on improving along with the modern era. In this modern intelligent world, almost everyone has a smart device such as smartphone and etc. These smart devices can emit signal thus RFID devices are prone to different signal distortions from the environment. Hence, many studies have been carried out to design a RFID tag that is able to overcome different distortion caused by different environment. A lot of researches also have been carried out to design a RFID antenna with a high gain, read distance and power transmission coefficient.

1.3 Aims and Objectives

The objectives of this project are:

- To design an UHF RFID tag antenna for a metal-mountable applications in the UHF RFID band.
- To study the properties of the tag antenna.
- To design a tag antenna that is able to function perfectly in different environments and conditions.
- To design a tag antenna that has high gain, long read distance as well as good impedance matching.
- To design a tag antenna that meets the global RFID pre-requirements.

Gain	≤ -3 dB
Resonant Frequency	Between 0.86 GHz to 0.96 GHz
Power Transmission Coefficient	≥ 0.7
Read Distance	≥ 10 m
Microchip Used	Monza 5

Table 1. 1: Pre-requirements in designing the RFID tag antenna

1.4 Thesis Organisation

Chapter 1 briefly discusses about the background of the radio-frequency identification tag as well as the aims and objectives of the project.

Chapter 2 briefly discusses on the antenna parameter. Besides that, it also discusses about literature review on how to enhance the antenna gain, bandwidth, impedance matching, read distance and power transmission of the antenna.

Chapter 3 discusses on the design methodologies and work flow on the design process of the RFID tag antenna. It also describes the 2-D and 3-D configurations of the tag antenna.

Chapter 4 focuses on the results collected from the project and explains the collected measured results compared to the simulated results.

Chapter 5 summarises and concludes this projects, followed by some recommendations that need to be carried out for future works.

CHAPTER 2

LITERATURE REVIEW

2.1 Introduction

The design process of RFID tag is a difficult task since many factors need to be considered. Hence, a study of relevant knowledge about the RFID tag had been carried out to design a perfectly working RFID tag antenna.

2.2 Antenna Parameter

There are a few antenna parameters that we need to take care about. Those parameters include radiation efficiency, antenna gain, S-parameter, bandwidth as well as the resonance frequency. Each of these parameters will heavily affect the performance and properties of the antenna.

2.3 Radiation Efficiency and Antenna Gain

Radiation efficiency is a measure of the electromagnetic energy radiating from an antenna. It is the measure on how well an antenna can convert radio-frequency electrical signal into radiated power.

Antenna gain is how well an antenna can direct the electromagnetic energy towards a particular direction. Many wireless communication devices suffer losses in term of radiation efficiency and gain due to the surrounding objects that will absorb some of the radiating energy and convert it to heat energy and causing a decrease in the efficiency and gain **(Sangaran et al., 2016)**.

2.4 UHF RFID Frequency Band Allocation

Universally, each nation has its unique frequency band allocation for UHF RFID application. Table 1.1 below shows the frequency allocation in the UHF RFID application for different nations **(Chen et al., 2009)**.

Country	Frequency Band
Malaysia	919 MHz ~ 928 MHz
China	840.5 MHz ~ 844.5 Hz and 920.5 MHz and 924.5 MHz
America	902 MHz ~ 928 MHz
Europe	866 MHz ~ 869 MHz
Singapore	866 MHz ~ 869 MHz and 920 MHz ~ 925 MHz
Japan	952 MHz ~ 955 MHz

Table 2. 1: Frequency band allocation for different nation in the UHF RFID application.

2.5 Resonant Frequency

A radio frequency antenna is consist of inductive and capacitive elements which determine the resonant frequency. Resonant frequency is found when the capacitive reactance and inductive reactance cancel each other. The antenna's size is strongly correlates to the antenna's resonant frequency. The larger the antenna, the lower the resonant frequency. Figure below illustrates on where is the resonant frequency located at.

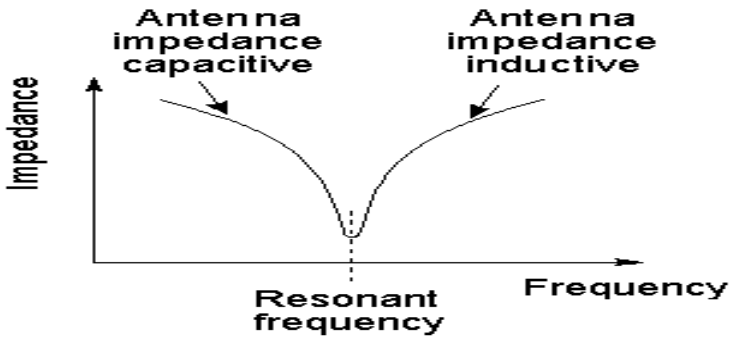

Figure 2. 1: Resonant frequency location when the capacitive reactance and inductive reactance cancel each other.

2.6 S-parameter and Bandwidth

Scattering parameters (S-parameters) is a technique to evaluate the performance of a system in terms of reflection and transmission of power. It is dependent on the number of port of the system. There will be 4 parameters to be considered in a two port systems which are S_{11}, S_{12}, S_{21} and S_{22}. Each parameter carries its own description. Assuming that Port 1 is the input while Port 2 represents the output, then S_{21} is insertion loss while S_{12} is reverse isolation. For instance, if S_{21} is 0 dB, it means that the power is fully transmitted from Port 1 and is completely received by Port 2. If S_{21} is -10 dB, then 1 W of power supplied to Port 1 will then be received by Port 2 at 0.1 W. On the other hand, S_{11} and S_{22} represent the reflection coefficient because it represent the power reflected from the load back to its own source. Thus, when S_{11} is said to be 0 dB, then all the power is fully reflected without any power being transmitted. All of these S-parameter can be represented in mathematical form.

$$\Gamma_{\text{in}} = S_{11} \tag{2.1}$$

$$\Gamma_{\text{out}} = S_{22} \tag{2.2}$$

$$IL = -20\log_{10}|S_{21}| \text{ dB} \tag{2.3}$$

$$I_{\text{rev}} = \left|20\log_{10}|S_{12}|\right| \text{ dB} \tag{2.4}$$

Where

Γ_{in} = Reflection coefficient (input port).

Γ_{out} = Reflection coefficient (output port).

IL = Insertion loss.

I_{rev} = Reverse isolation.

The antenna's bandwidth is the working frequency range of the antenna. The bandwidth is strongly related to the S-parameter since the bandwidth of the antenna can be found in the S-parameter curve. Frequencies range for S_{11} below -10 dB are considered as the bandwidth of the antenna. Figure below illustrates how bandwidth of an antenna can be found from the S-parameter curve.

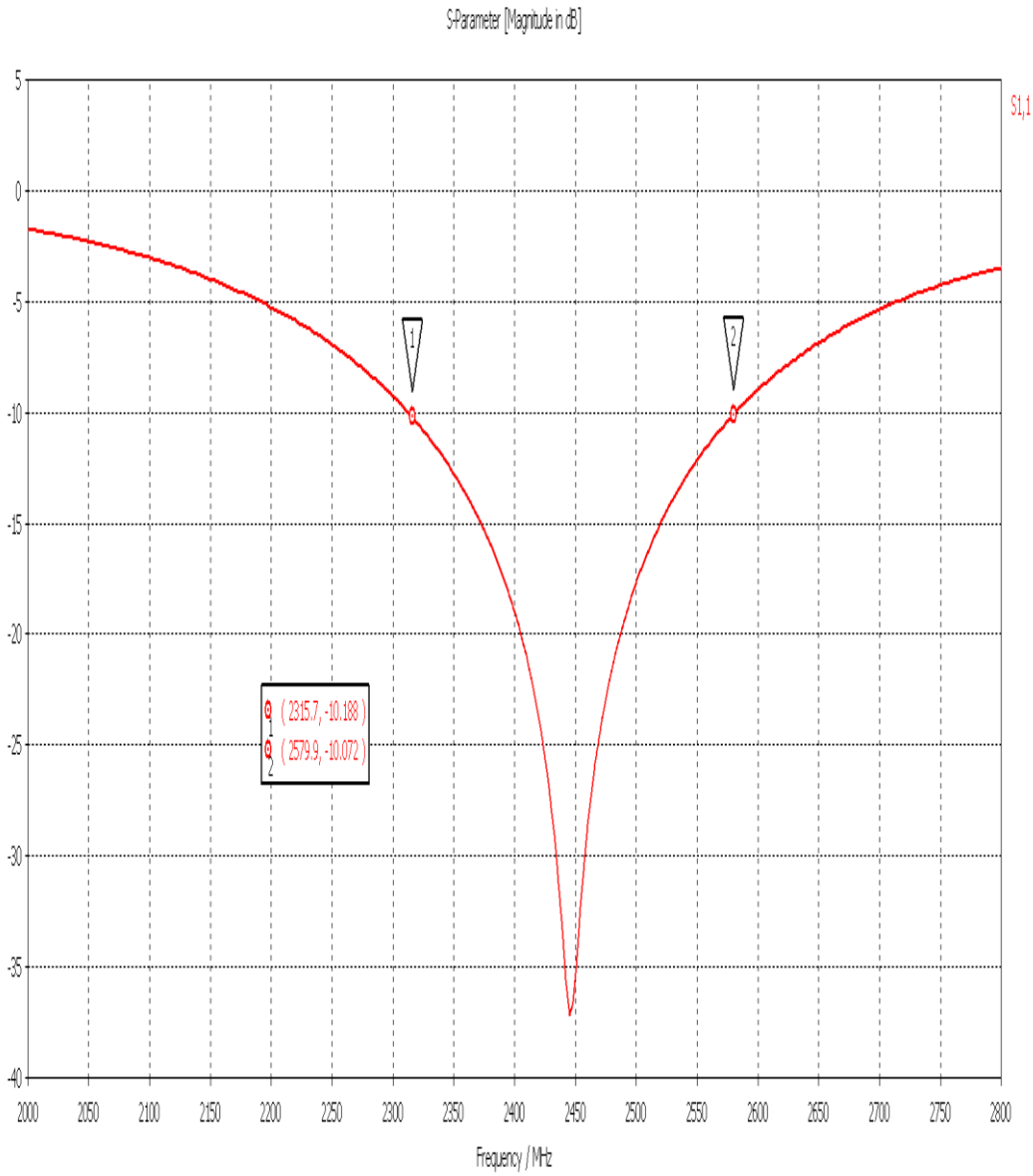

Figure 2. 2: The bandwidth of an antenna found from the S-Parameter curve.

2.7 Read Range of the Antenna

Read range is define as how far in term of distance a signal emitted from a tag antenna can be received and identified by the tag reader **(Rao et al., 2015)**. Read distance is relatively important for a tag antenna. The longer the read distance of a tag antenna, the easier the signal emitted from a tag antenna to be received by the tag reader.

The read range of the antenna can be calculated and obtained by using the Friss Formula for free space:

$$r_{\text{tag}} = \frac{\lambda}{4\pi}\sqrt{\frac{P_t G_t G_r \tau}{P_{\text{th}}}} \quad (2.5)$$

Where

r_{tag} = Read range

λ = Wavelength

P_t = Transmitting power of reader

P_{th} = Sensitivity of tag

G_t = Gain of the tag antenna

G_r = Gain of the reader

τ = Transmission coefficient

Read range can be affected by many factors. For instance, the orientation of the tag antenna, the material on which the tag antenna is attached to and the electromagnetic wave characteristics in different environments. Thus, various factors that will affect the read range of the antenna should be taken into consideration during the design process.

2.8 Review on How to Choose the Manufacturing Material of the Antenna

The materials used to manufacture the antenna are relatively important since every material has different conductivity and performance. Traditionally, etched copper and aluminium are used to construct antennas. Etching is a subtractive procedure that utilizes the synthetic substances and it can makes squander. Recently, most of the antennas are constructed by silver ink. However, silver ink has many disadvantages. One of the disadvantages is silver ink suffer from relatively low conductivity. Besides that, it will also cause environmental issues. These issues led to development of newer technologies like vapour-deposited aluminium and electro-less deposited copper.

There has been movement where highly-conductive copper is stacked onto a PET layer. This copper additive process can significantly minimize the wastage as well as reducing the environmental issues. From a research, they found out that the conductivity of the silver ink is much lower than copper (which is only 1/10 conductivity of copper). Besides that, the research also states that the performance of aluminium is almost the same as the copper. However, aluminium requires more thickness to achieve the same performance with copper. From the above results, we can conclude that copper is highly recommended for manufacturing antenna since it has high conductivity and much less deposited material (thinner) compared to other materials **(Huang et al., 2008)**.

Table below shows the conductivity and skin depth for different materials.

Material	Conductivity $(S/m) \times 10^6$	Skin Depth (μm) at 915 MHz
Bulk copper (BC)	58	2.18
Deposited copper (DC)	50	2.35
Bulk silver	61.8	2.1
Bulk Aluminium	36	2.8
Silver ink A	5.1	7.31
Silver ink B	4.2	8.11

Table 2. 2: Conductivity and skin depth for different materials.

2.9 Review on Methods to Enhance the Realized Gain of the Antenna

The realized gain of the antenna is always an issue during the design phase. The gain of the antenna depends on its size compared to wavelength. It is found that the aperture type antennas have a higher gain compared to other types of antennas **(Harrington, 1960)**.

Another method is using a stacked microstrip antenna which consist of two parasitic elements. From the experimental study, the gain of antenna will be increased by at least 3.7 dB ~ 5.7 dB by setting the parasitic element between the intervals of 0.25 λ ~ 0.35 λ onto the fed element. By doing this, the bandwidth of the antenna will also be increased **(Egashira et al., 1996)**.

Furthermore, another method to increase the gain is by stacking up a layer of superstrate into the substrate. This is a resonance gain method by using a superstrate method **(Jackson et al., 1985)**. Superstrate is a kind of material that will increase the gain of the antenna and without changing the resonant frequency of **a**ntenna **(Qiang et al., 2008)**. To further increase the gain, the thickness of the antenna can be increased through the addition of number of superstrate layers **(Yang et al., 2018)**.

Other than that, gain can be increased by using photonic band gap (PBG) technique. It is a technique that enclose the patch antenna with a square lattice of tiny metal plates with grounding vias. By doing this, massive suppression of surface waves will excite the substrate result in increasing of gain **(Qian et al., 1998)**. Figure below illustrates the PBG technique.

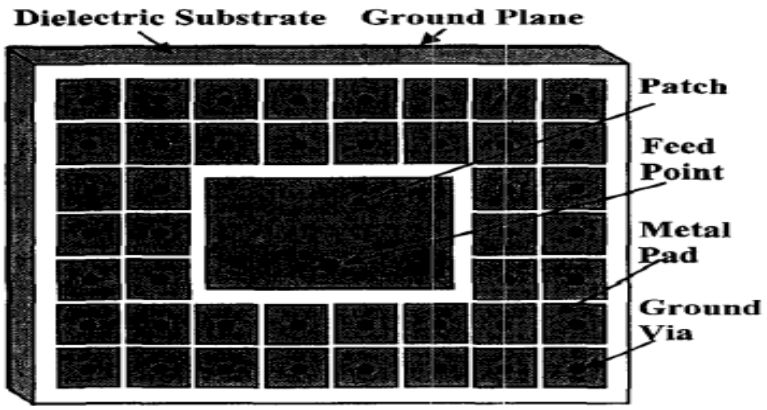

Figure 2. 3: PBG lattice technique on microstrip antenna.

2.10 Review on Ways to Broaden the Bandwidth of the Antenna

Narrow bandwidth is always an issue for many microstrip antenna. There are several methods on increasing the bandwidth of antenna. The most common way is using a relatively thick substrate. This is because thicker substrate has lower Q factor which result in broader bandwidth. However, this method will support surface waves which results in deterioration of the radiation patterns and causing the decrease in radiation efficiency **(Pozar, 1992)**.

Besides that, broadband impedance matching is also a method to increase the bandwidth. This method is used since it does not change the radiating element by itself. A reactive matching network is included to reimburse the frequency fluctuations of the input impedance **(Pues et al., 1989)**. On the other hand, adding more resonant elements like patches and feedline into the antenna can also increase the bandwidth **(Abdelaziz, 2006)**.

There are some other examples of increasing the bandwidth of an antenna. For instance, a U- shaped slot applied onto the patch has successfully broaden the bandwidth **(Sze et al., 2000)**. Another example is from **(Liu et al., 2015)** in which two coin-shaped patches surrounded with a ring shape strip has successfully enhance the bandwidth. Figure 2.4 below illustrate how the U –shaped slot look like while figure 2.5 shows how the two coin-shaped patches look like.

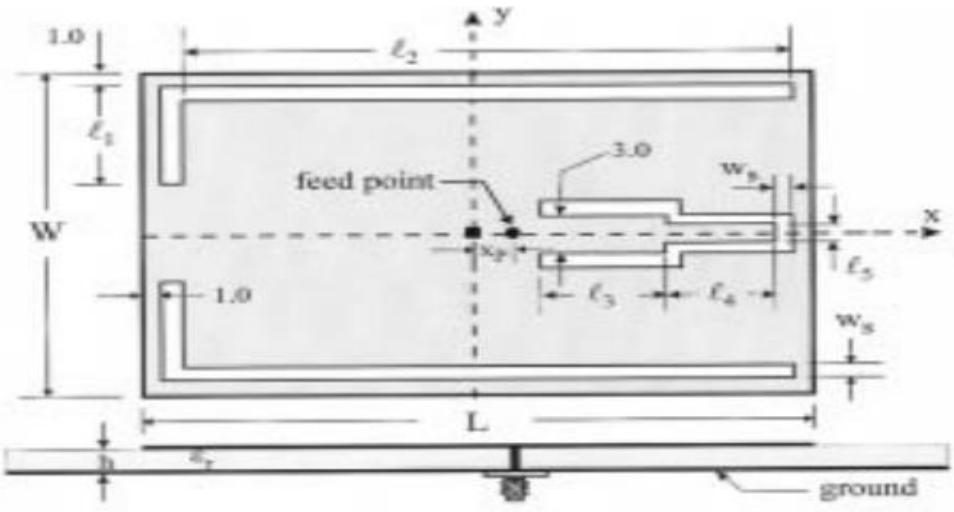

Figure 2. 4: U-shaped slot on the patch.

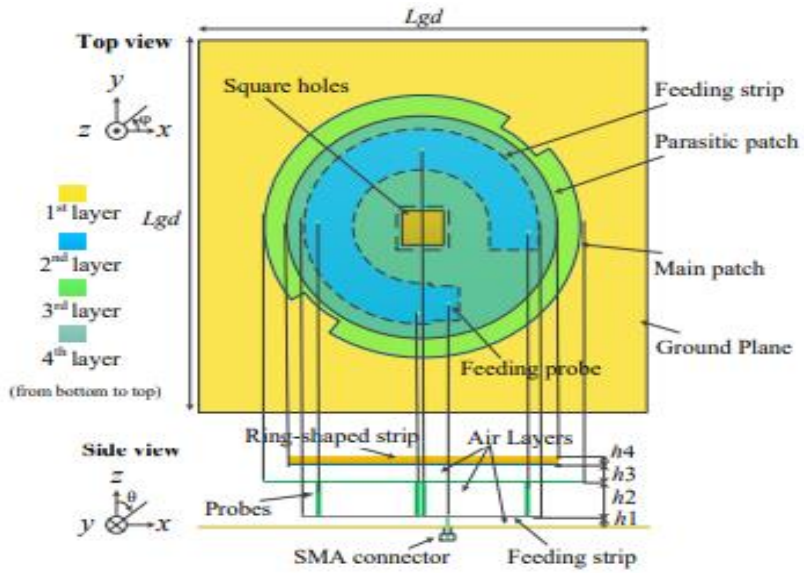

Figure 2. 5: Two coin-shaped patches.

2.11 Review on Factors that will affect the Resonant Frequency Shift of the Antenna

During the design phase, tuning the frequency to the desired range is always a difficult task. Hence, several studies had been carried out to tune the frequency. There are several factors that will cause the shifting of resonant frequency in an antenna. The first factor that will affect the resonant frequency is the size of the patch antenna. The larger the physical size of the antenna (length), the lower the resonate frequency **(Trembly, 1985)**. This can be explained from equation 2.6 below.

$$f = \frac{c}{\lambda} \tag{2.6}$$

Where

f = Frequency.

c = Speed of light $(3 \times 10^8 \text{ m/s})$.

λ = Wavelength.

Usually, wavelength is considered in determining the length of antenna. From the above equation, we know that frequency is inversely proportional to the wavelength. Hence, we can conclude that the larger the antenna patch size (in term of length), the smaller the resonant frequency. Other than that, increases in the overall size of the patch antenna will also increases the inductance of the antenna and result in lower resonant frequency.

Another factor that will affect the resonant frequency is the dielectric constant, ε of the material. Generally but not all cases (since it is depending on the temperature), the dielectric constant decreases as the frequency increases **(Yadav, 2010)**. Figure below shows the graph of the dielectric loss versus frequency for copper.

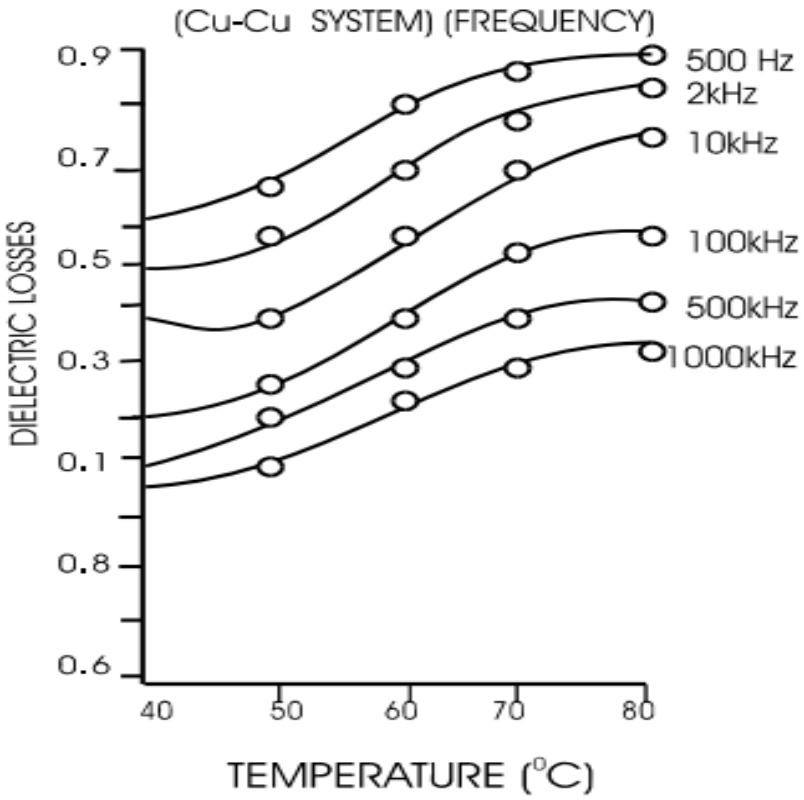

Figure 2. 6: Graph of the dielectric loss versus frequency for copper.

2.12 Review on Impedance Matching of the Tag Antenna

Impedance matching is very important for designing an antenna since poor impedance matching will result in poor power transfer. Besides that, poor impedance matching will also causing poor gain and narrow bandwidth. To achieve maximum power transfer between the chip and the antenna, impedance matching must be achieved between microchip and the tag antenna. Figure below illustrates the read range reaches a peak value when the impedance of antenna, X_a matches the impedance of microchip, X_c **(Rao et al., 2005)**.

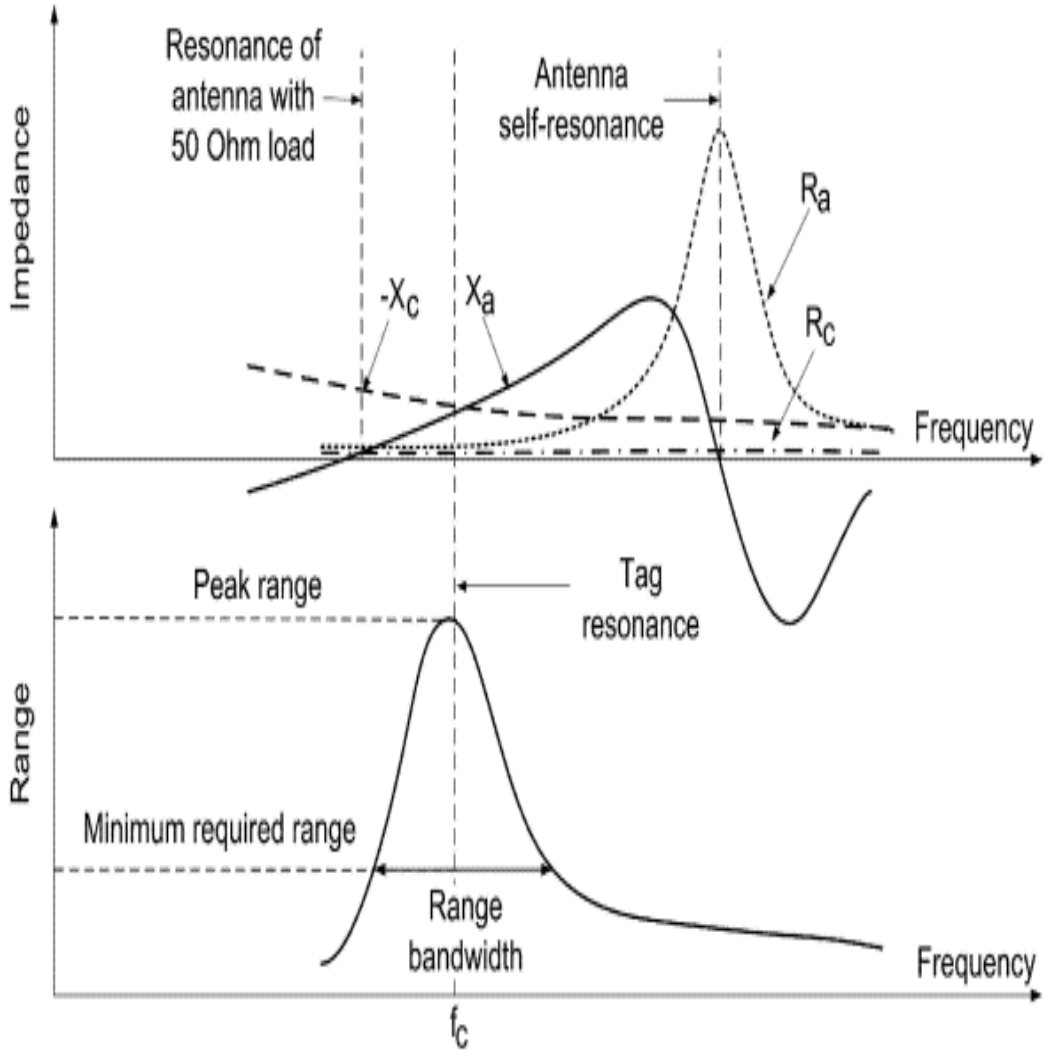

Figure 2. 7: Performance of the power transmission when impedance matching is happened.

One of the method to have a good impedance matching is using non-Foster impedance matching concept. This concept uses a group of passive elements such as inductors and capacitors to bypass the restriction of gain-bandwidth theory **(Sussman et al., 2009)**.

Another method to improve the impedance matching is by using an elliptical antenna. The axis of the elliptical current distribution will keep on changing with frequency and results in wider impedance match bandwidth **(Huang et al., 2005)**. Figure below shows how an elliptical antenna looks like.

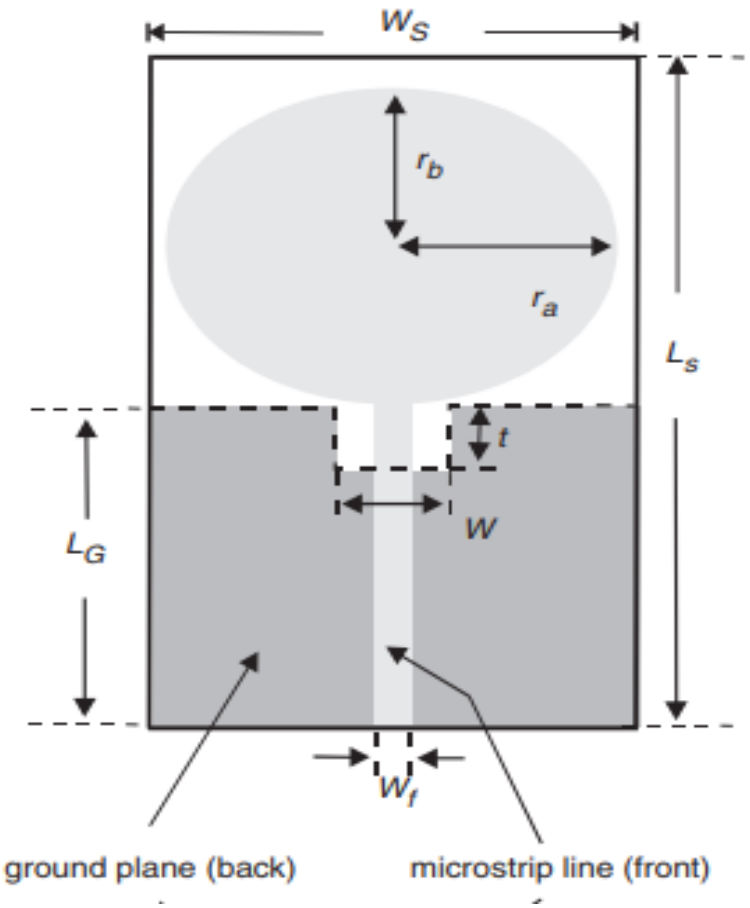

Figure 2. 8: An elliptical antenna.

CHAPTER 3

METHODOLOGY AND WORK PLAN

3.1 Introduction

The software used to design the tag antenna is CST Microwave Studio 2018. It is a powerful software in 3D electromagnetic simulation of high frequency components. CST help us to design RFID antenna, microstrip antenna and etc. Besides that, it also helps us to monitor the electric field distribution and the magnetic field distribution of the antenna. Moreover, it also allows us to monitor and calculate the surface current, S_{11}, impedance, power transmission coefficient and etc. All of the simulation and design processes of this project are completed using CST Microwave Studio 2018.

Voyantic Tagformance measurement system had been used to measure the performance of the prototype tag antenna. The performance parameters include read range, gain and etc of the tag antenna. To avoid interference, the tag antenna is inserted into an anechoic cabinet during the measurement.

3.2 Chip used in this Project

The chip applied in this experiment is Monza 5 tag chip. It has a high read sensitivity. The impedance of the Monza 5 tag chip is 14.56 – j161.25 Ω.

3.3 Dimension of the Tag Antenna

The tag antenna is designed to have a length of 45 mm, a width of 45 mm and a thickness of 3.379 mm.

3.4 Configuration of the Tag Antenna (Layer view)

The proposed tag antenna of this project is used for metal-mountable application. In this project, the overall design of the tag antenna is made up by 3 layers of conductive patch and 2 layers of foam. The figure below shows the configuration (layer by layer) of the tag antenna in layer view.

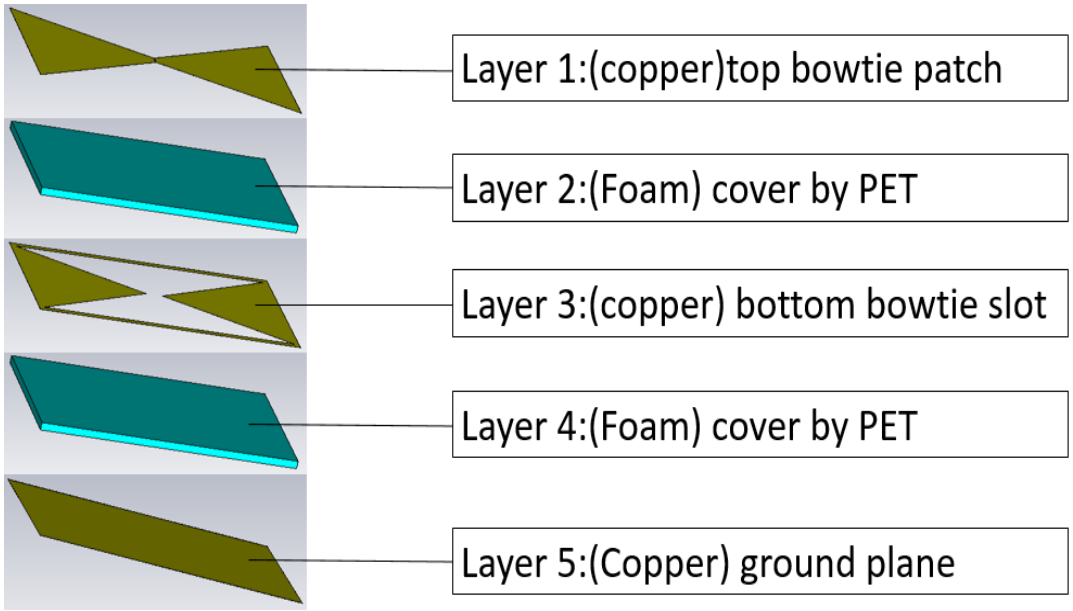

Figure 3. 1: Configuration of the tag antenna (layer by layer)

3.5 3-D Configuration of the Tag Antenna

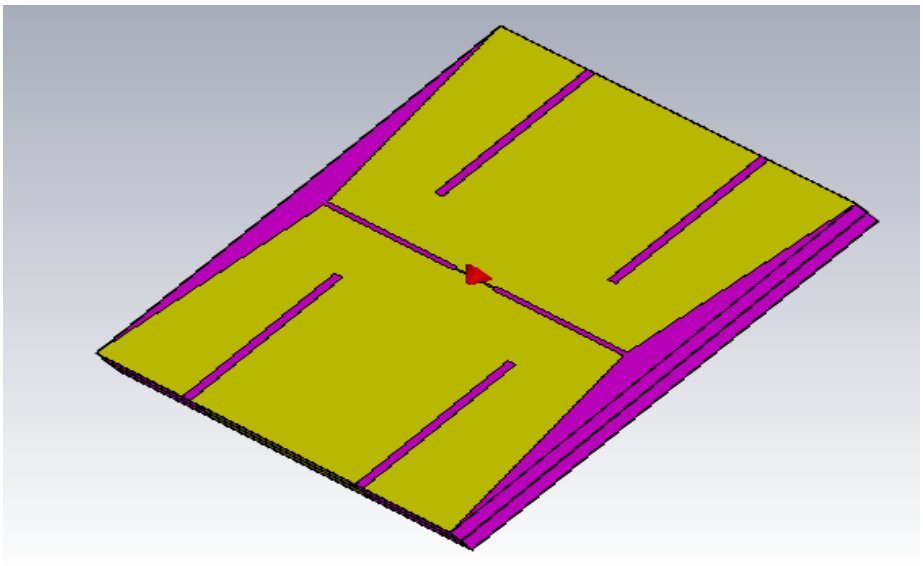

Figure 3. 2: 3-D configuration of the tag antenna.

3.6 2-D Configuration of the Tag Antenna.

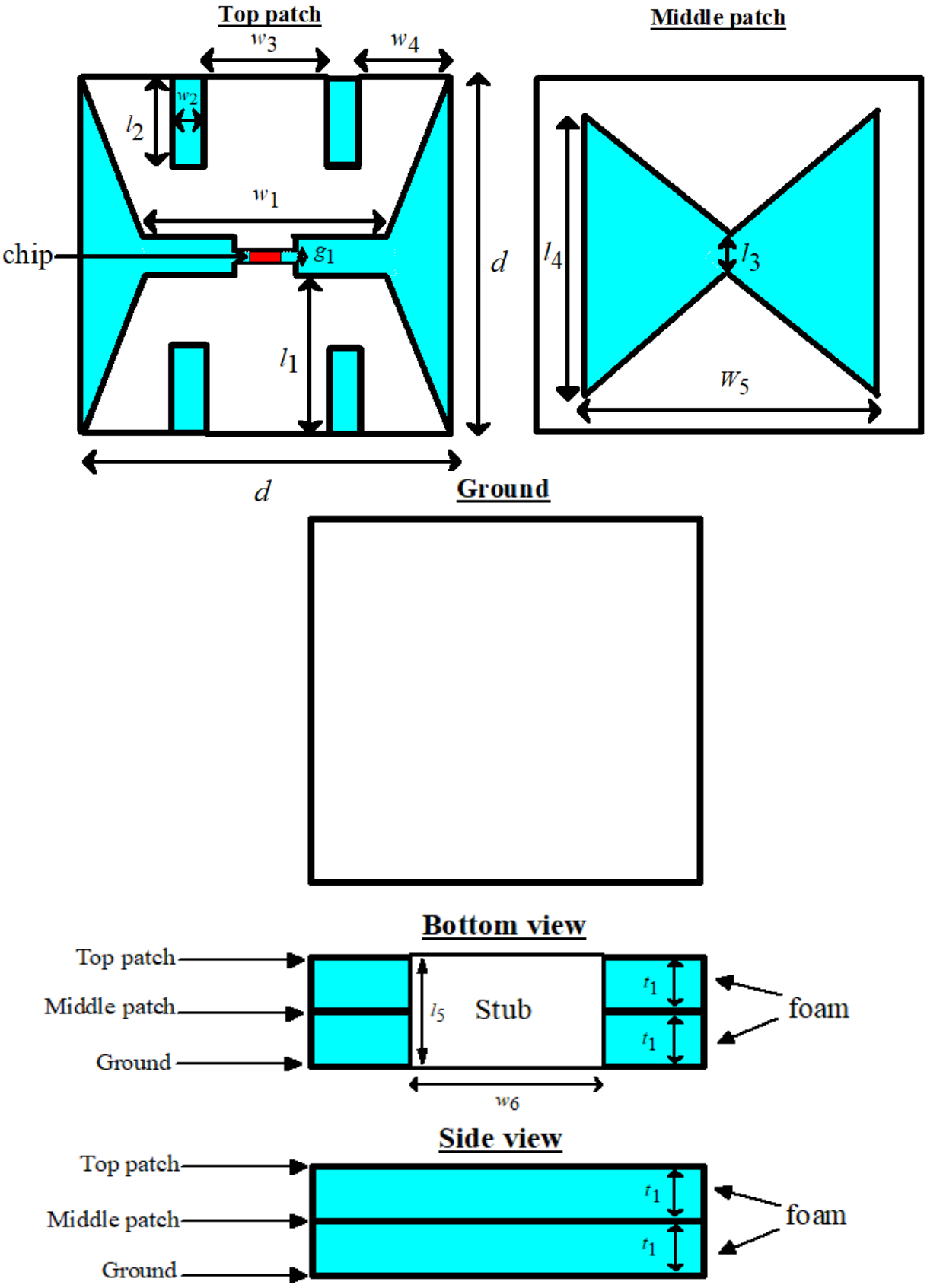

Figure 3. 3: 2-D configuration of the antenna.

3.7 Parameters and Values.

Symbol	Value (*mm*)
d	45
w_1	38
w_2	1
w_3	21
w_4	11
w_5	40
w_6	20
l_1	22
l_2	17
l_3	6
l_4	40
l_5	3.379
t_1	1.6
g_1	0.15

Table 3. 1 : Parameters and values

3.8 Location of Monza 5 Chip.

The Monza 5 chip is placed at the centre of the top patch. Figure below shows the location of the Monza 5 chip.

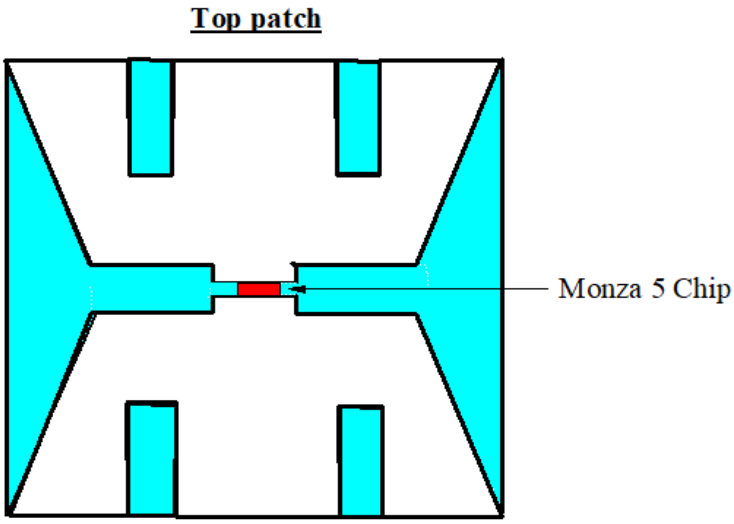

Figure 3. 4: Location of Monza 5 chip.

3.9 Prototype

Figures below show the prototype of this project.

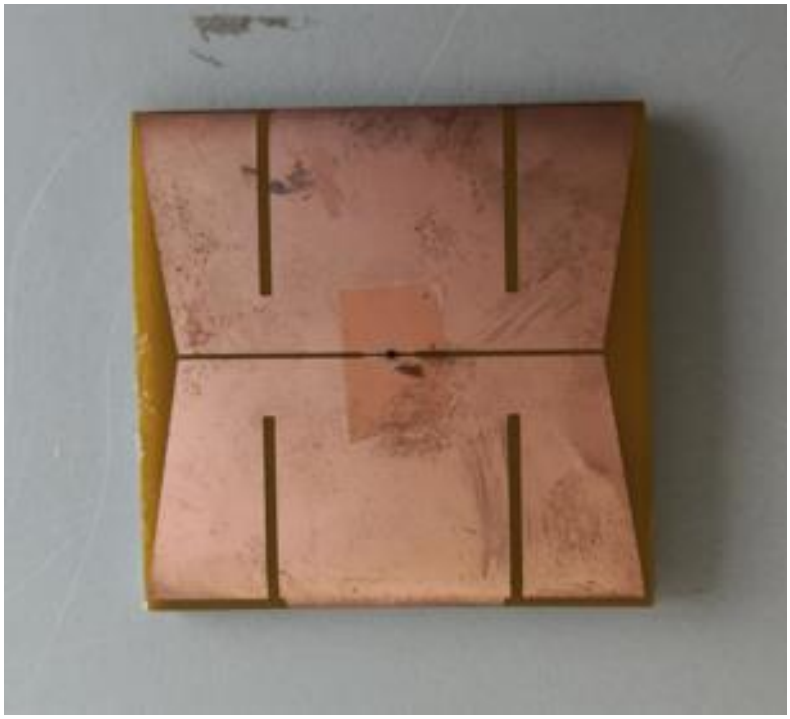

Figure 3. 5: Overview prototype for the top patch.

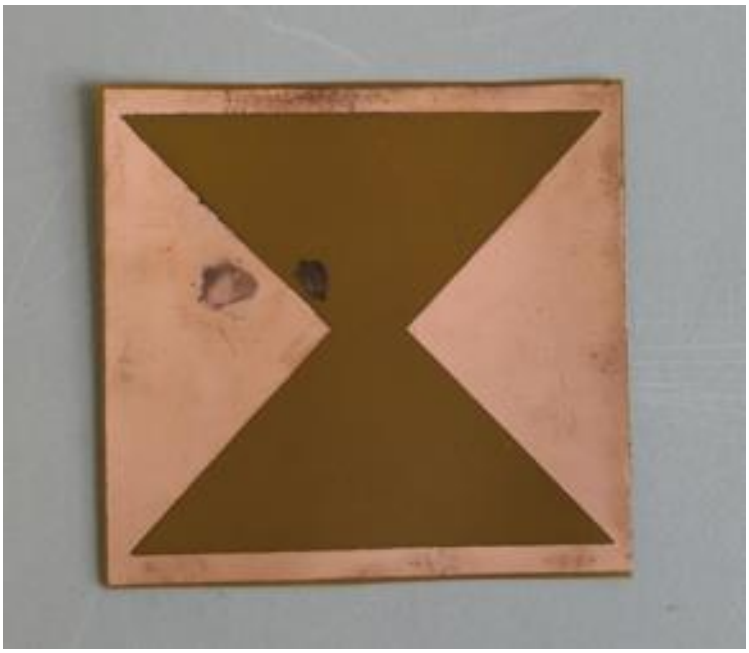

Figure 3. 6: Overview prototype for the middle patch.

3.10 Measurement Setup

The performance of the tag antenna is measured by using Voyantic Tagformance system inside an anechoic cabinet. Figure below illustrates the measurement setup of the tag antenna.

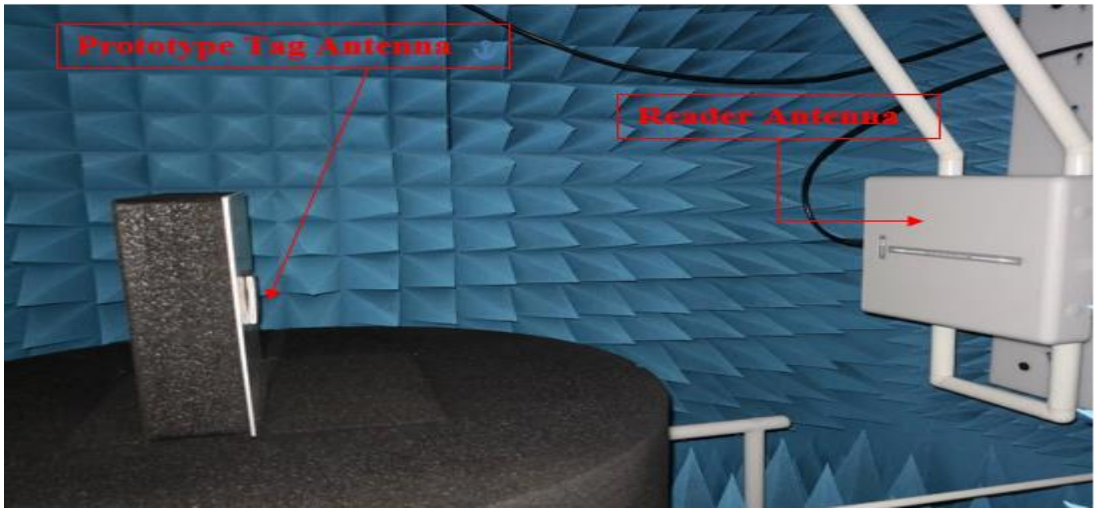

Figure 3. 7: Measurement setup.

From figure 3.7, the reader antenna is in the fix location and this reader antenna is used to measure the performance of the prototype tag antenna for y-z plane. Beside y-z plane, the tag antenna also must be measured for x-y plane as well as x-z plane. Hence, the tag antenna is placed under three different reader antenna in different locations to measure the performance of the tag antenna in x-y, x-z, and y-z plane. Figure below illustrates how the tag antenna is measured for x-y, x-z, and y-z plane.

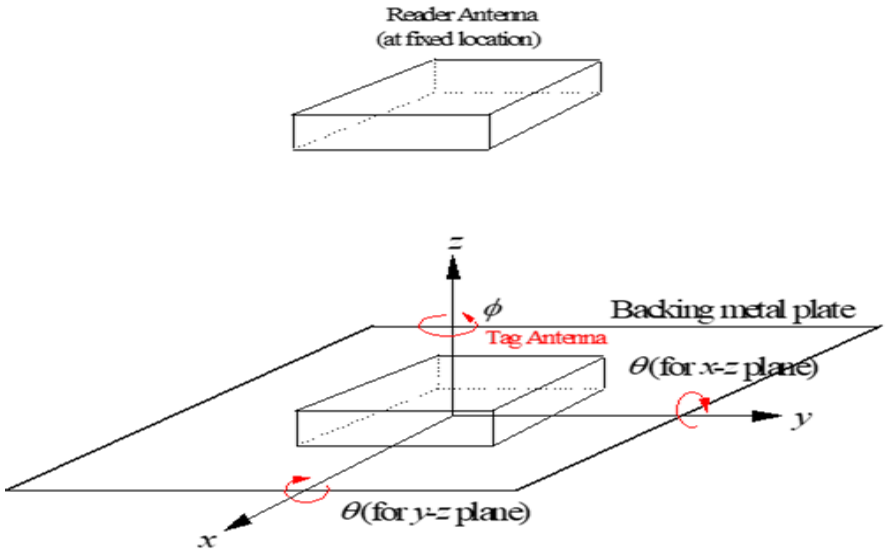

Figure 3. 8: Tag antenna measured for x-y, x-z, and y-z plane.

3.11 Fabrication

Flowchart below shows the process of fabrication.

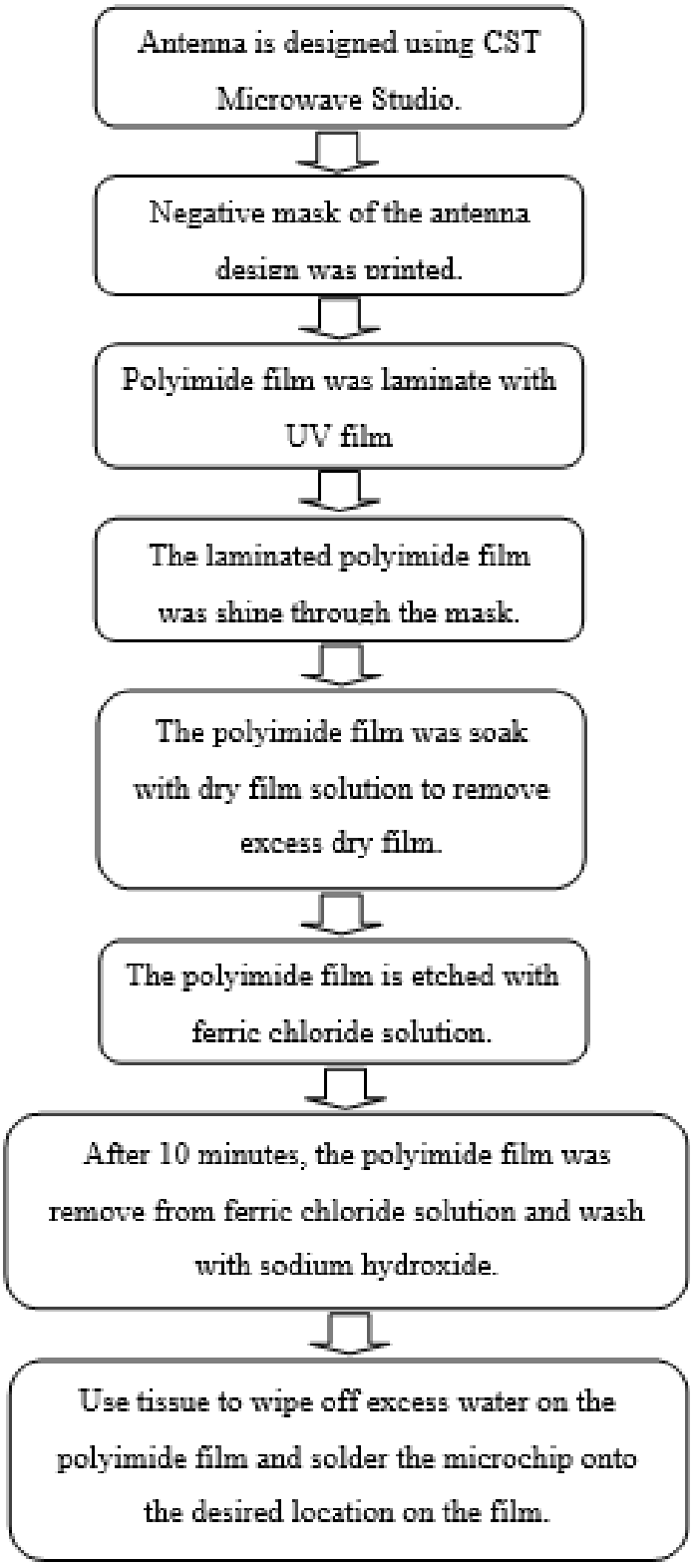

Figure 3. 9: Flowchart for the fabrication of the tag antenna.

3.12 Summary

Flowchart below illustrates the overall process of this project.

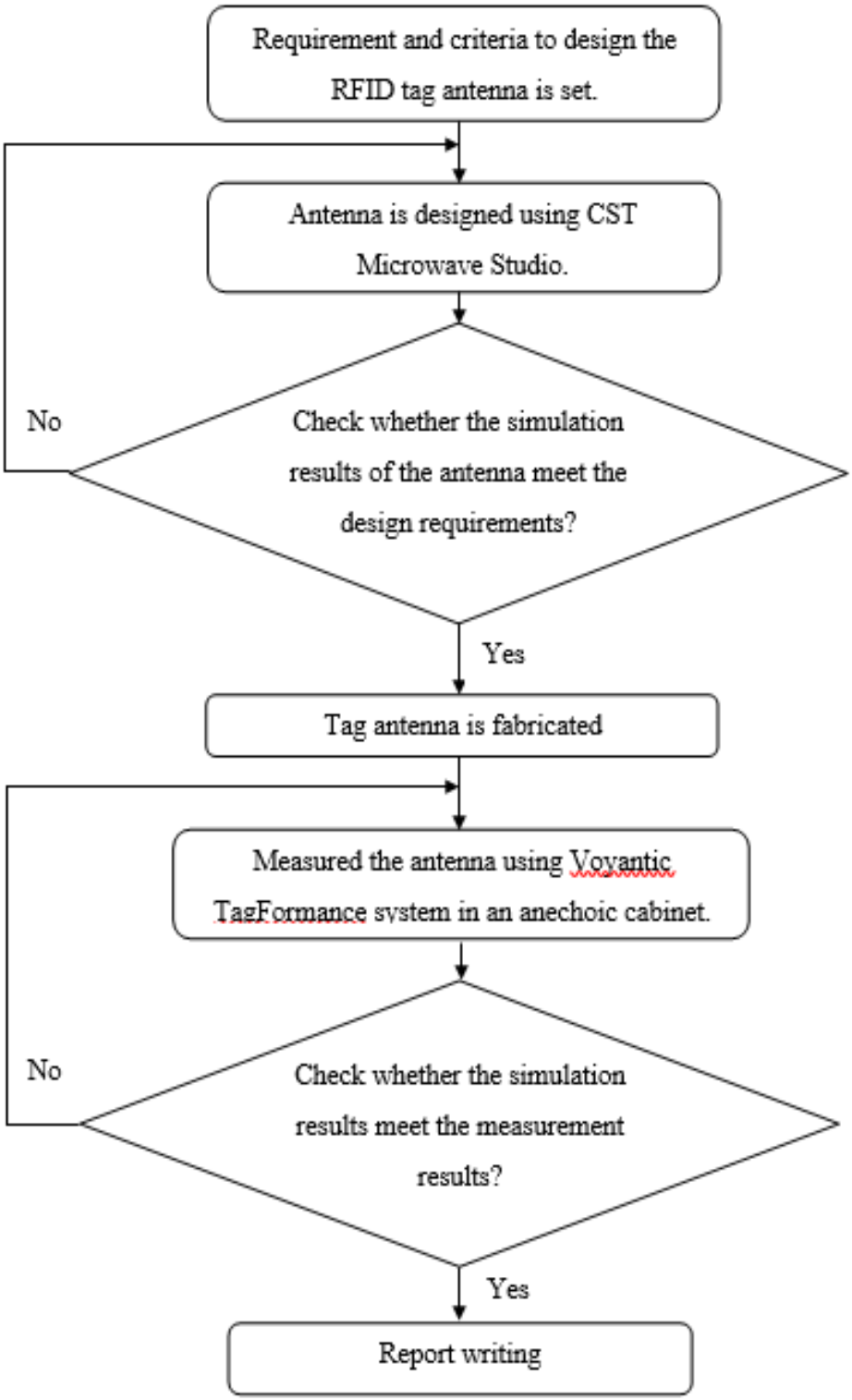

Figure 3. 10: Flowchart for overall process of this project.

CHAPTER 4

RESULTS AND DISCUSSIONS

4.1 Simulation Results of the RFID Tag Antenna by using CST MWS

All the simulated results are collected from CST Microwave Studio 2018.

4.1.1 Simulated Reflection Coefficient and Resonant Frequency

Figure below shows the graph of the simulated s-parameter (S_{11}) and the simulated resonant frequency.

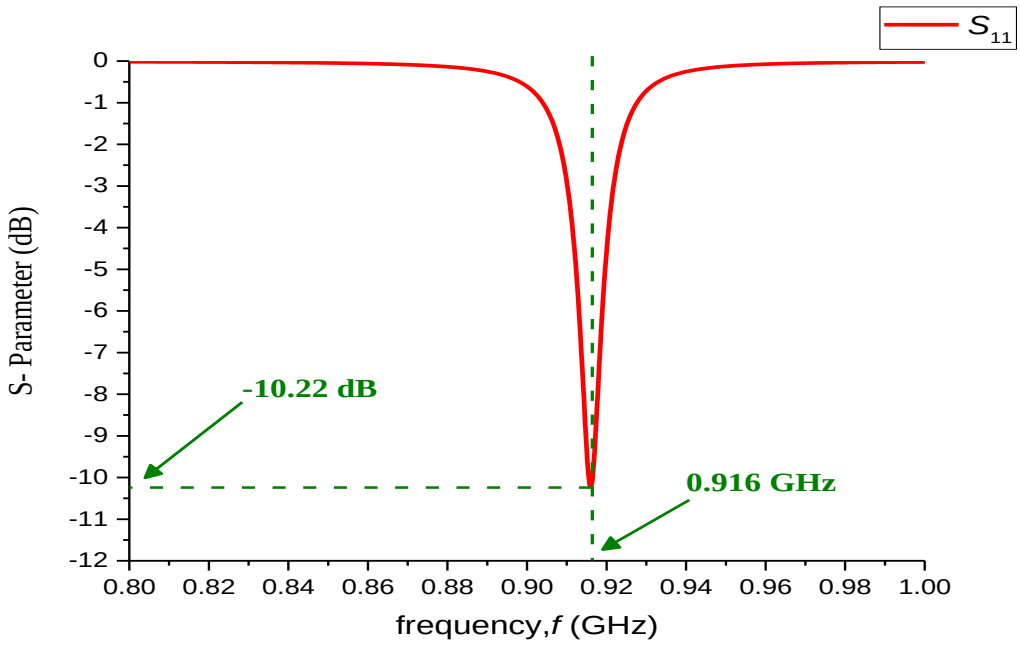

Figure 4. 1: Graph showing the simulated reflection coefficient, S_{11} and simulated resonant frequency.

From the above graph, the simulated resonant frequency of the tag antenna is *0.916 GHz* which complies with the universal UHF RFID frequency band between 0.860 GHz ~ 0.960 GHz. The simulated reflection coefficient, S_{11} of the tag antenna is -10.22 dB. This results shows that the impedance matching is achieved between the chip and the antenna.

4.1.2 Simulated Input Impedance

Figure 4.2 shows the real part simulated input impedance, while figure 4.3 shows the simulated input impedance for imaginary part.

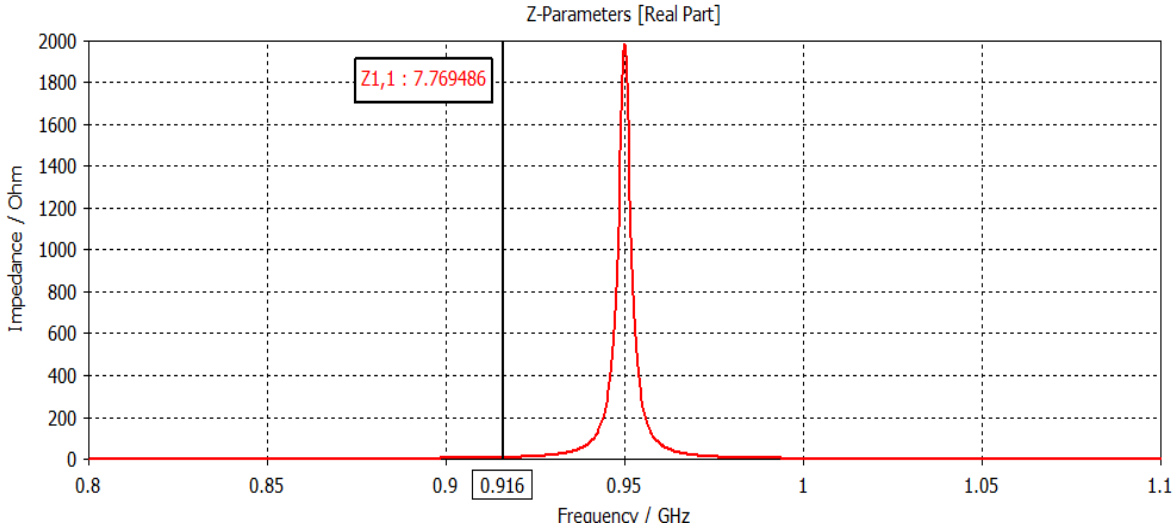

Figure 4. 2: Simulated input impedance (Real part).

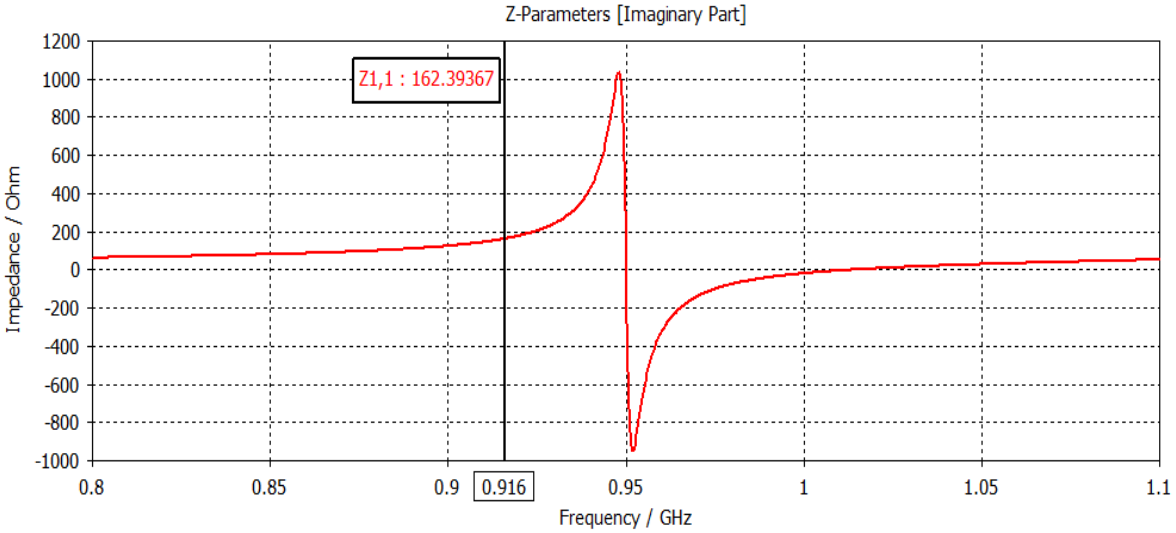

Figure 4. 3: Simulated input impedance (Imaginary part).

From the above results, the simulated real input impedance for the antenna is 7.77 Ω while the simulated imaginary input impedance is j162.39 Ω. The total simulated input impedance (real + imaginary) is 7.77 Ω + j162.39 Ω. Meanwhile, the input impedance of the Monza 5 chip is 14.56 – j161.25 Ω. This shows that good impedance matching is attained and maximum power transfer between the Monza 5 chip and the antenna is achieved.

4.1.3 Simulated Power Transmission Coefficient

Good matching and maximum power transfer achieved between the tag antenna and the Monza 5 chip can be further proven from the below figure. Figure below shows the simulated power transmission coefficient of the antenna.

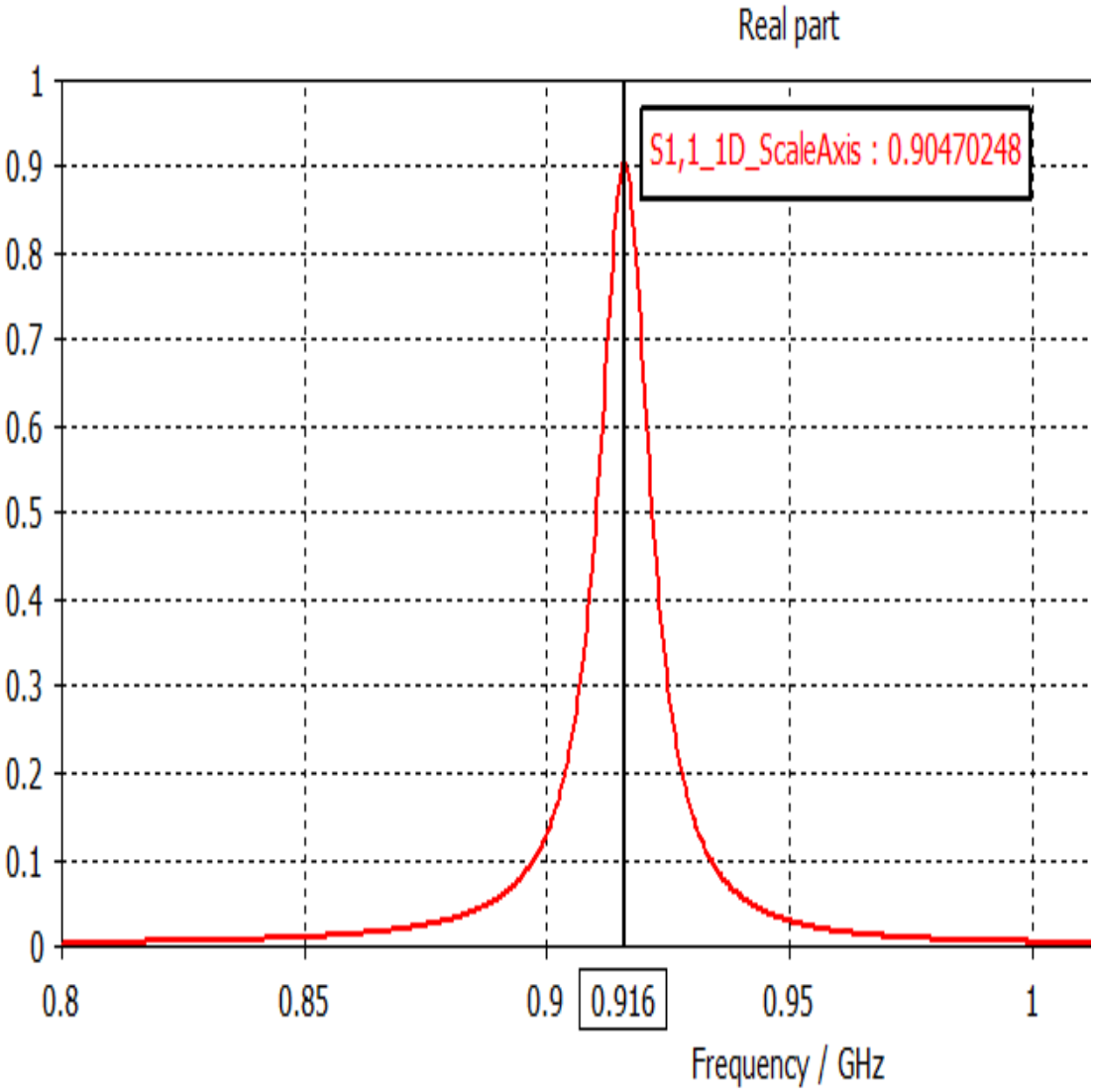

Figure 4. 4: Simulated power transmission coefficient.

From the above graph, the simulated power transmission coefficient is 0.9047. The power transmission efficiency is 0.9047 x 100 % = 90.47 %. With this high power transmission efficiency, it proves that good matching is achieved between the tag antenna and the chip.

4.1.4 Parametric Analysis of the Tag Antenna.

A few changes of crucial parameters on the antenna will affect the behaviours as well as the properties of the tag antenna. Hence, some parametric analyses have been carried out in order to understand the changes in the performance of the tag antenna.

Firstly, the length of the slot on the top patch, l_2 has been changed from 15 mm to 20 mm with a constant step size of 1.25 mm. Figure 4.5 below shows the effect of varying parameter l_2 on the power transmission coefficient.
From the results, the resonance frequency shifts gradually from 0.908 GHz to 0.919 GHz when l_2 is decreased from 20 mm to 15 mm. Reducing the length of slot, l_2 will reduce the capacitance of the antenna thus increases the resonant frequency of the antenna. From the graph below, it is clear that the average simulated power transmission coefficient is maintain at around 0.90, meaning the impedance of the antenna is conjugate matched with the chip impedance.

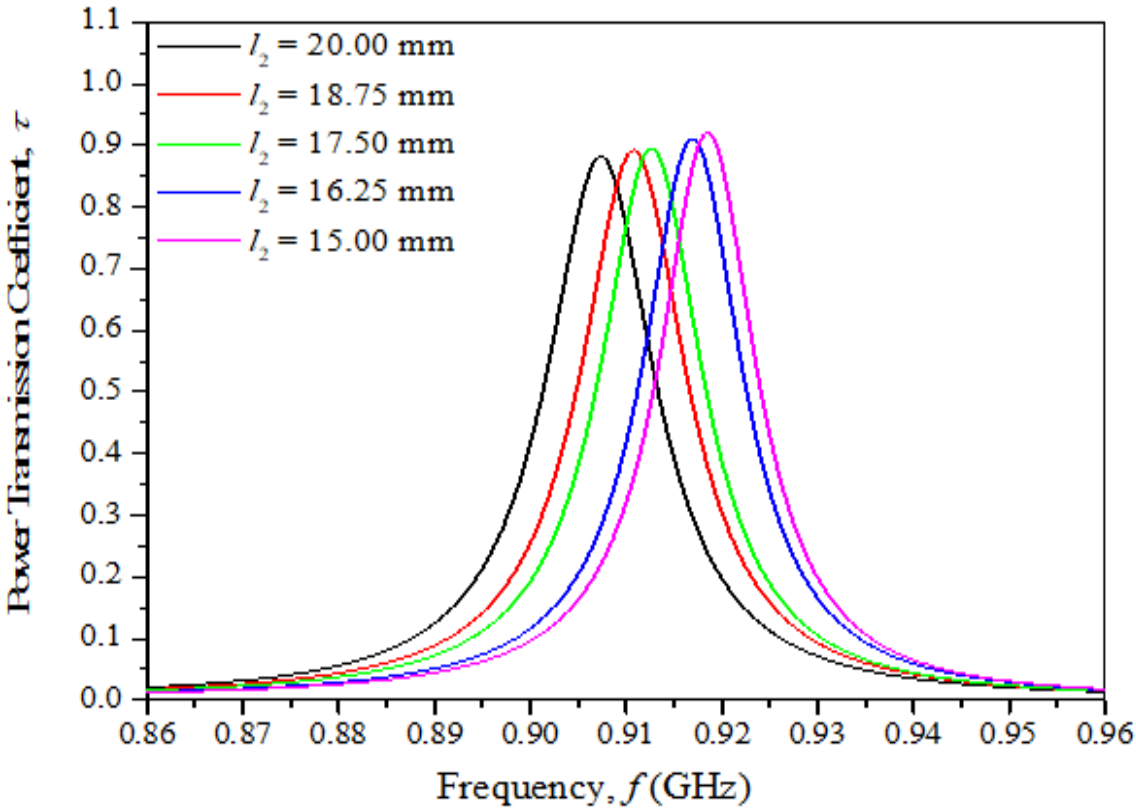

Figure 4. 5: Parametric analysis on varying parameter l_2, (power transmission coefficient).

From figure 4.6, the resistance and reactance become lower in value when l_2 decreases gradually. This is because reducing in l_2 will decreases the inductance of the antenna and results in decreasing in input impedance. Inductive reactance is directly proportional to inductance. This statement can be proven from the equation below. Equation below shows the relationship between inductive reactance and inductance.

$$X_L = \frac{V}{I} = \Omega \mathrm{L} \tag{4.1}$$

Where

X_L = Inductive reactance

V = Voltage

I = Current

L = Inductance

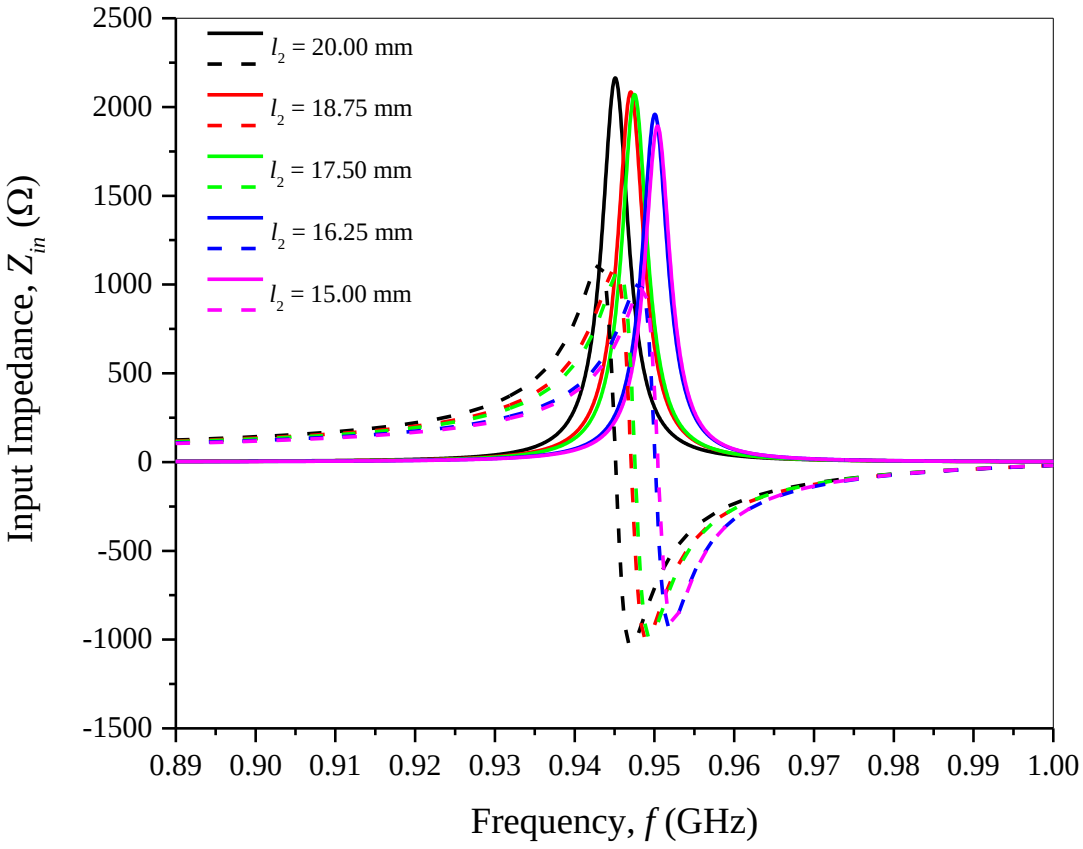

Figure 4. 6: Parametric analysis on varying parameter l_2, (input impedance).

Next, the width of the stub connecting top patch to the ground, w_6 has been changed from 19.10 mm to 21.90 mm with a constant step size of 0.45 mm. Figure 4.7 below shows the effect of varying w_6 on the power transmission coefficient. It shows that the resonance frequency shifts gradually from 0.908 GHz to 0.921 GHz when w_6 is increased from 19.10 mm to 20.90 mm. When the stub width w_6 increases, the inductance will decrease, results in increasing in resonant frequency of the antenna. From the graph below it is clear that the average simulated power transmission coefficient is maintain at around 0.91. As usual as the above scenario, conjugate match between the impedance of the antenna and the chip is achieved.

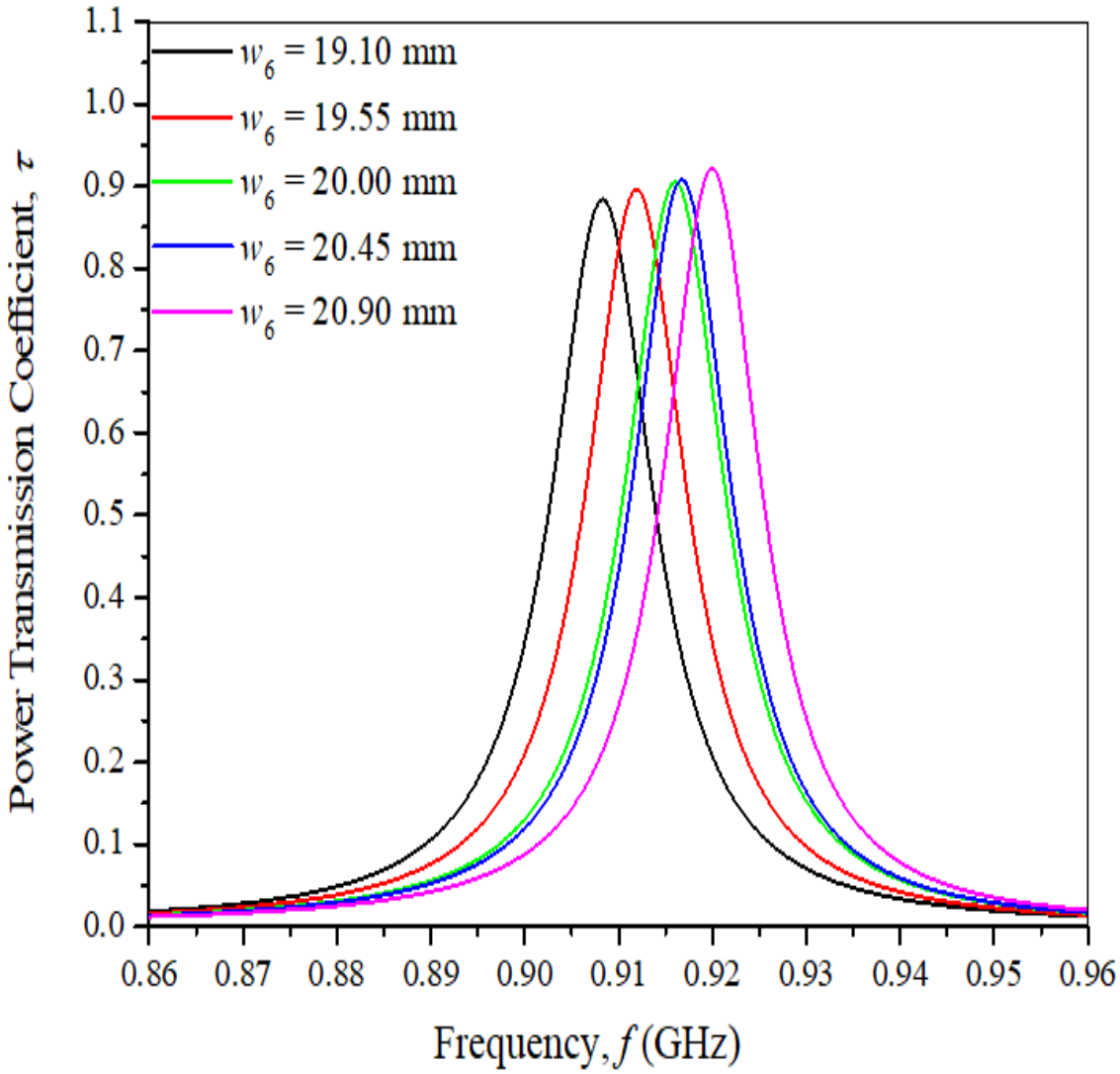

Figure 4. 7: Parametric analysis on varying parameter w_6, (power transmission coefficient).

From figure 4.8, the resistance and reactance decrease when the width of the stub, w_6 increases gradually. This is because reducing in w_6 will decrease the inductance of the antenna and results in decreasing in input impedance.

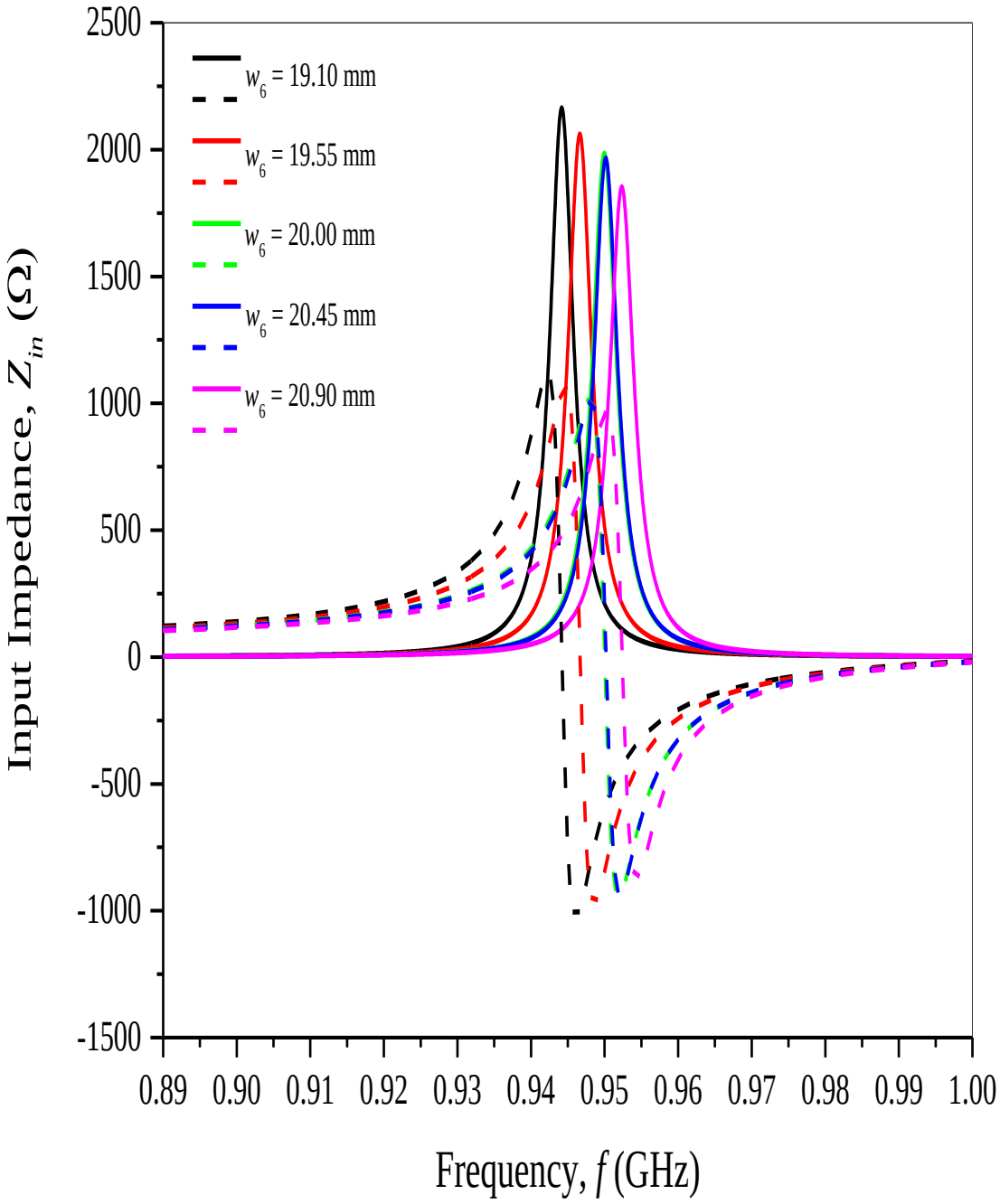

Figure 4. 8: Parametric analysis on varying parameter w_6, (input impedance)

The width of the slot on the middle patch, w_5 has also been taken into account for parametric analysis. The slot width, w_5 has been changed from 39 mm to 41 mm with a constant step size of 0.5 mm. Figure 4.9 below shows the effect of varying parameter w_5 on the power transmission coefficient. It shows that the resonance frequency shifts gradually from 0.880 GHz to 0.945 GHz when w_5 is decreased from 41 mm to 39 mm. Shorter slot width, w_5 will decrease the inductance of the antenna thus increases the resonant frequency of the antenna. From the graph below it is clear that the average simulated power transmission coefficient is 0.95. It proved that conjugate match between the impedance of the antenna and the chip is achieved.

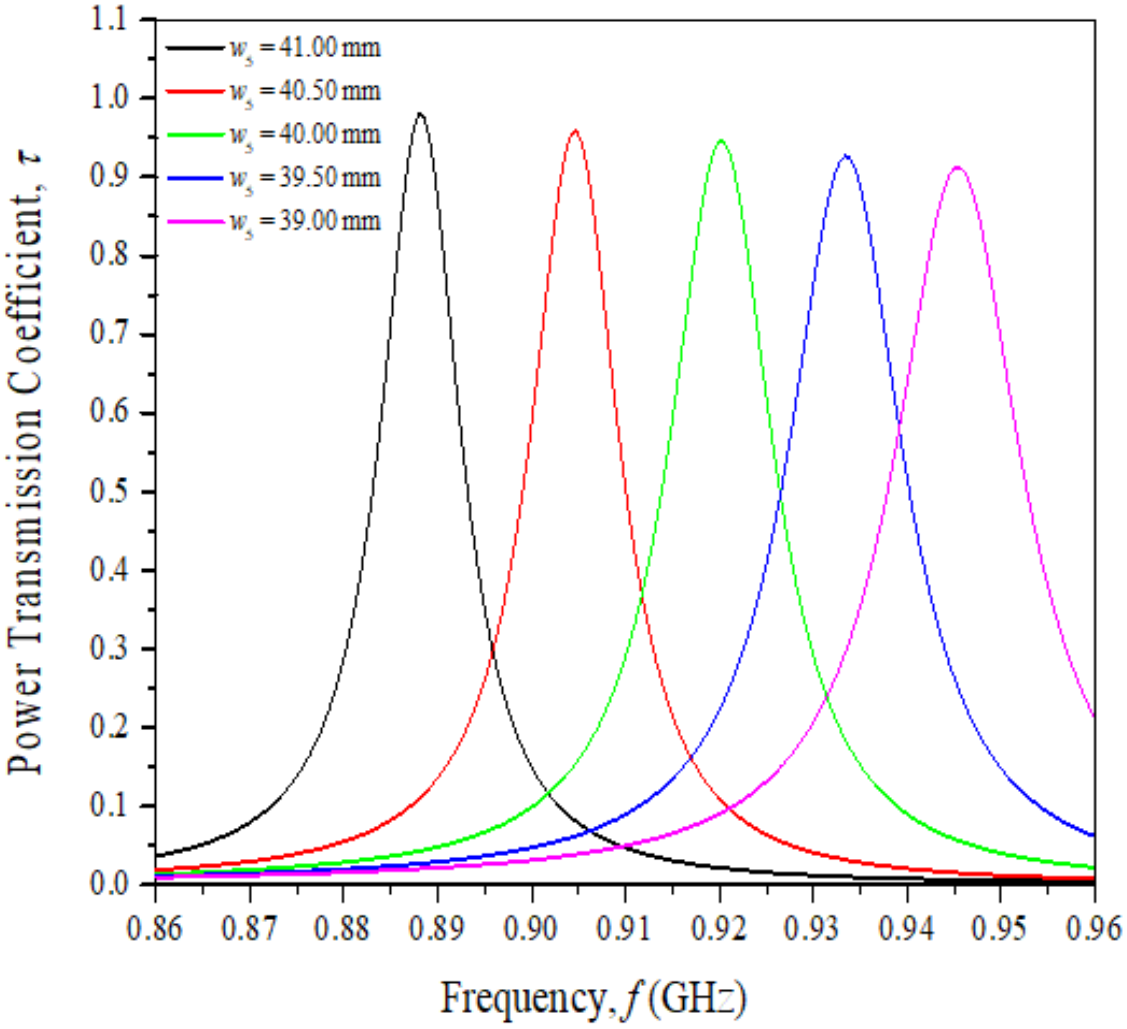

Figure 4. 9: Parametric analysis on varying parameter w_5, (power transmission coefficient).

From figure 4.10, the resistance and reactance increase when the width of the slot on the middle patch, w_5 decreases gradually. This is because reducing in w_5 will increase the inductance of the antenna and results in increasing in input impedance.

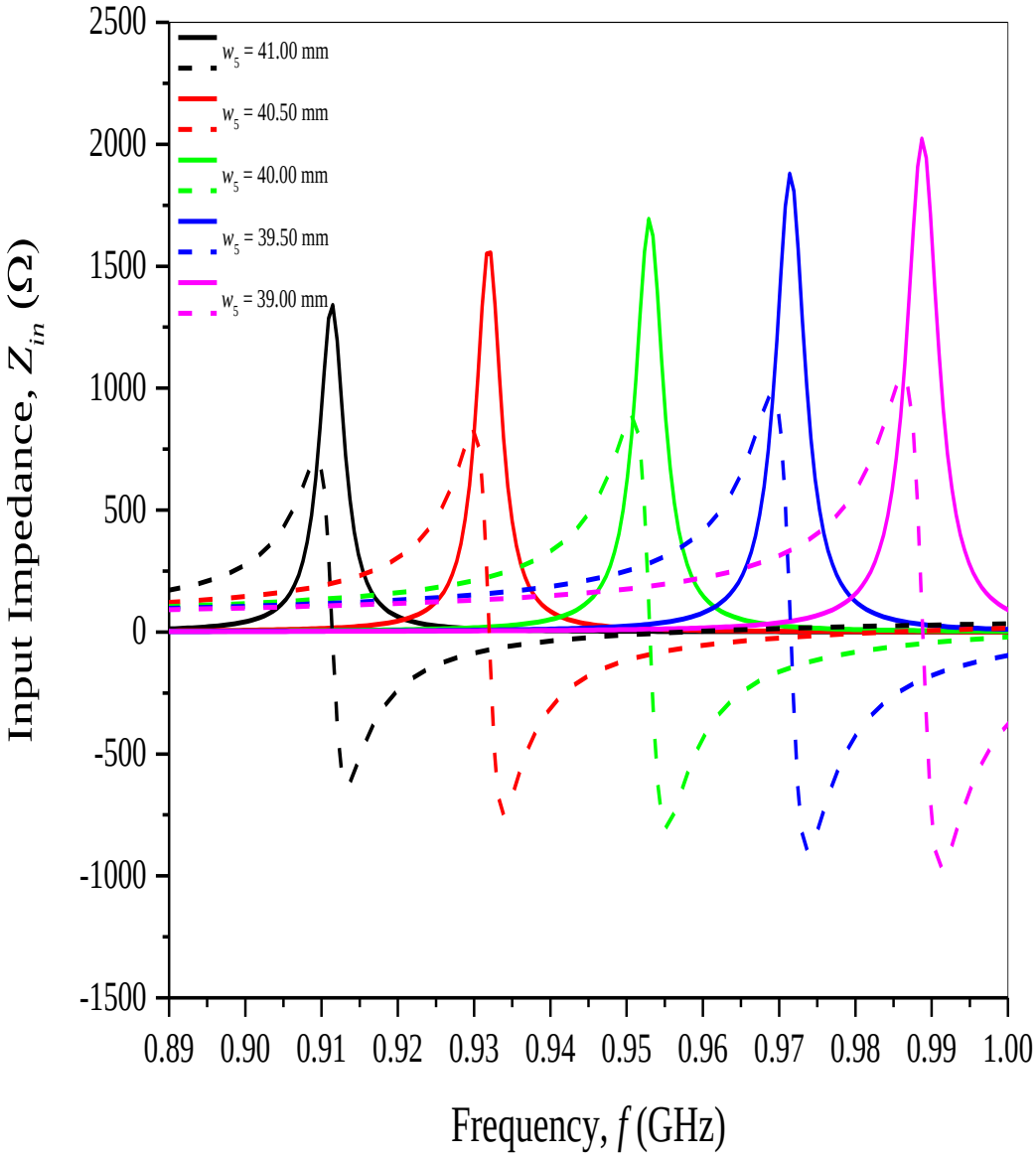

Figure 4. 10: Parametric analysis on varying parameter w_5, (input impedance).

4.1.5 Simulated Realized Gain

The simulated realized gain of the tag antenna is 2.554 dB. Figure below shows the simulated realized gain of the tag antenna.

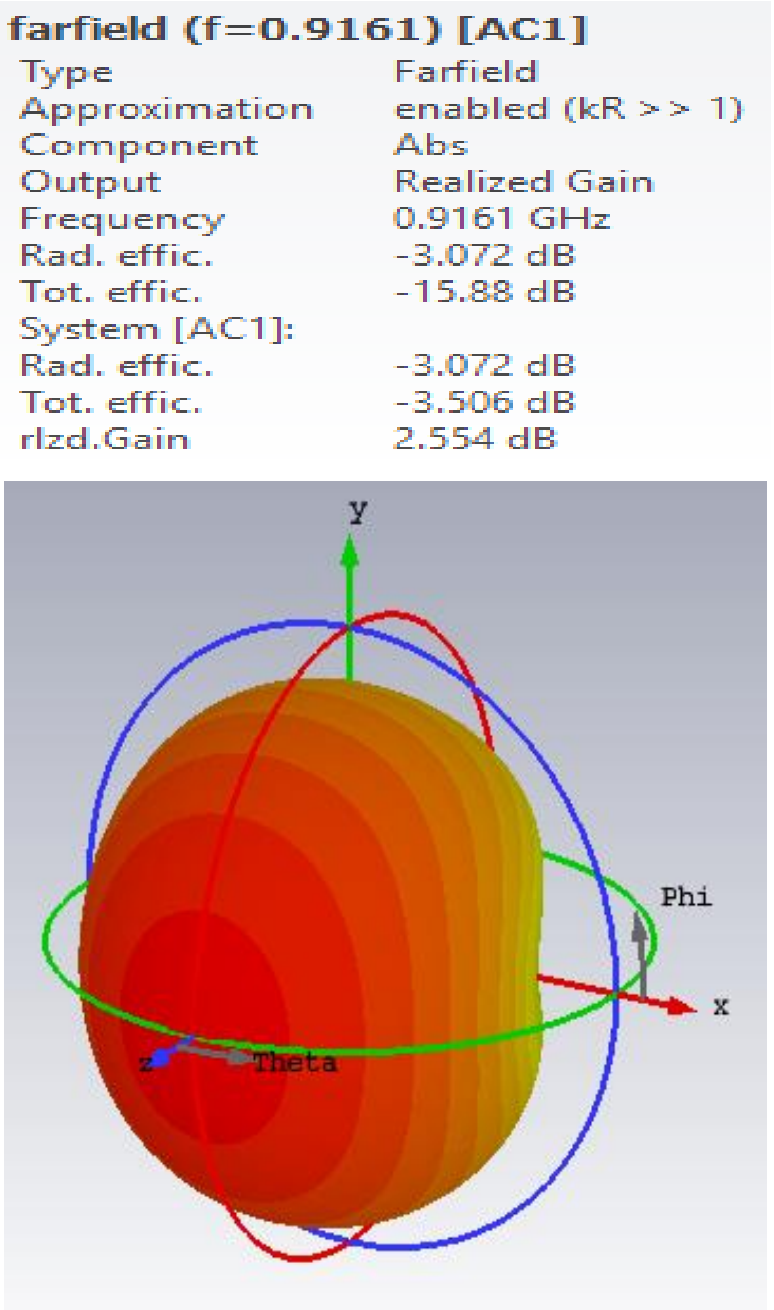

Figure 4. 11: Simulated realized gain of the tag antenna.

4.1.6 Electric Field Distribution

From the below figures, it show that the current flow from bottom towards top of the patch and create a current loop. The current at the centre of dipole is the strongest since the surface current distribution is densest at the centre. Figure 4.12 shows the electric-field distribution for top patch while figure 4.13 shows the electric-field distribution for middle patch.

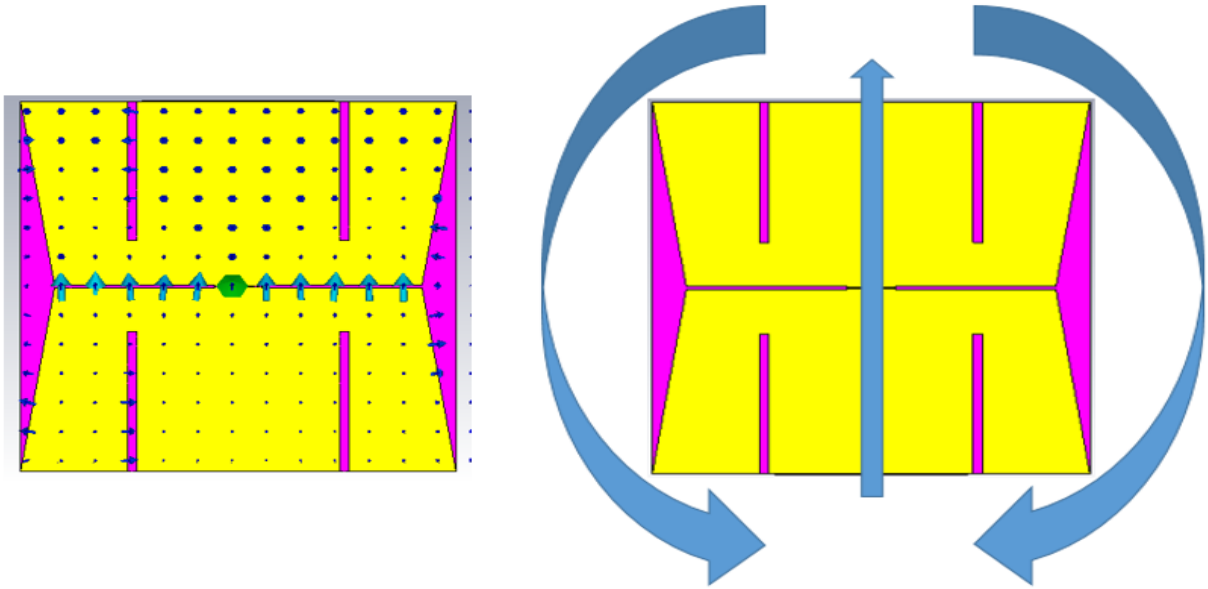

Figure 4. 12: Electric-field distribution for top patch.

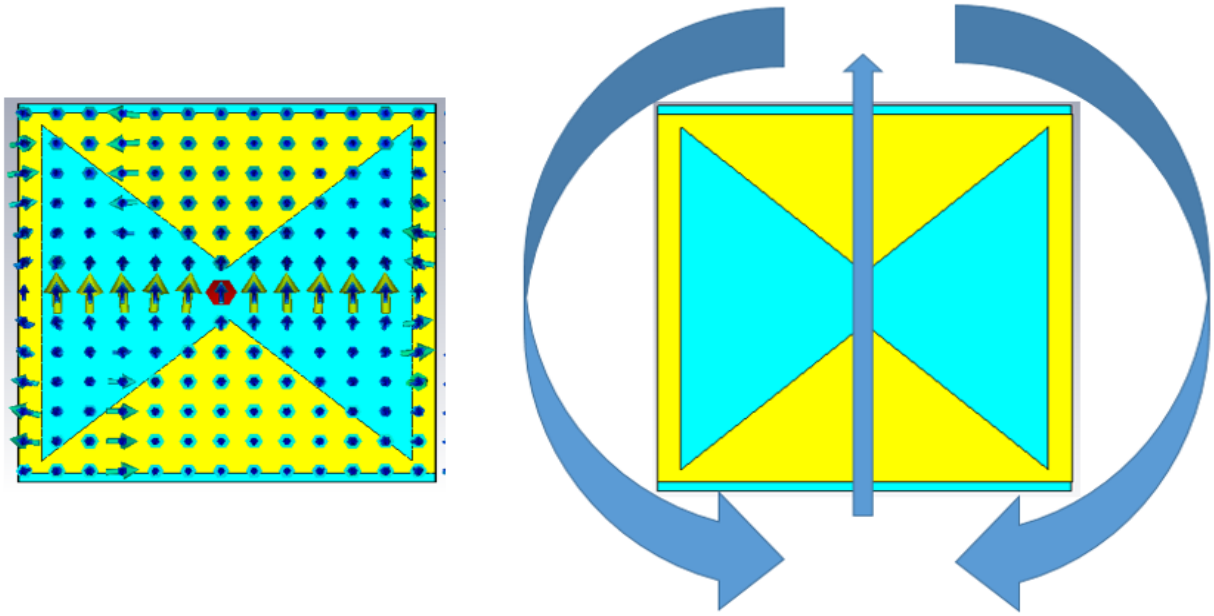

Figure 4. 13: Electric-field distribution for middle patch.

4.1.7 Magnetic Field Distribution

According to the Right hand grip rule, right thumb represents the direction of current while curl fingers represent the direction of magnetic field. The current is flowing from bottom to top of the dipole which mean the thumb is pointing upward. When the thumb is pointing upward, the curl fingers will curl to the right. Hence, the magnetic field flows from left to right which can show in figures below. Furthermore, the magnetic field at the centre of dipole is the strongest since the current at the centre is the strongest. Figure 4.14 shows the magnetic-field distribution for top patch while figure 4.15 shows the magnetic-distribution for middle patch.

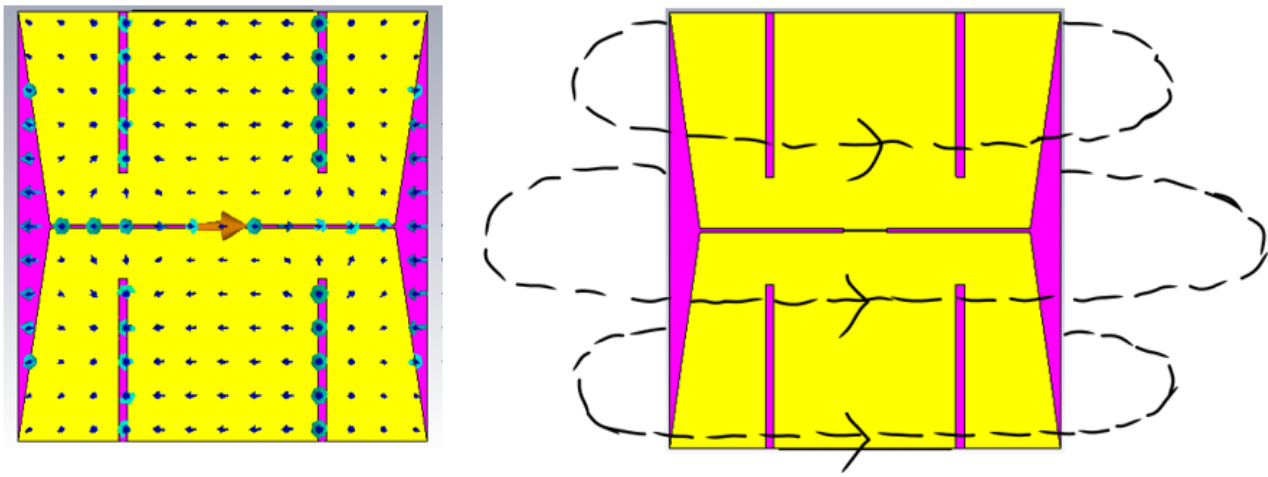

Figure 4. 14: Magnetic-field distribution for top patch.

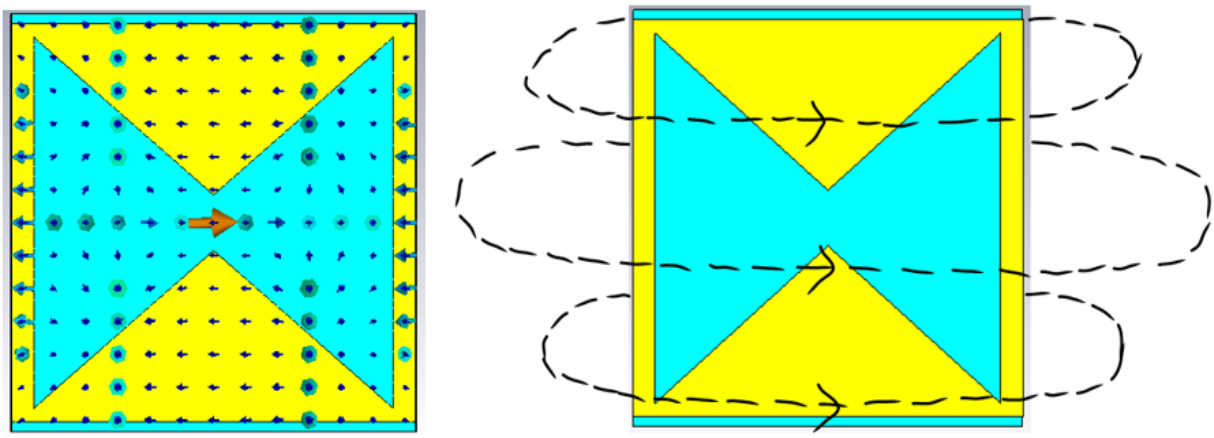

Figure 4. 15: Magnetic-field distribution for middle patch.

4.1.8 Surface Current Distribution

The current at the centre of dipole is the strongest since the surface current is densest at the centre. The current at the end of the patch is weaker since the surface current is less dense. Thus, the magnetic field at the end of the patch is weaker. Figure 4.16 shows the surface current distribution for top patch while figure 4.17 shows the surface current distribution for middle patch.

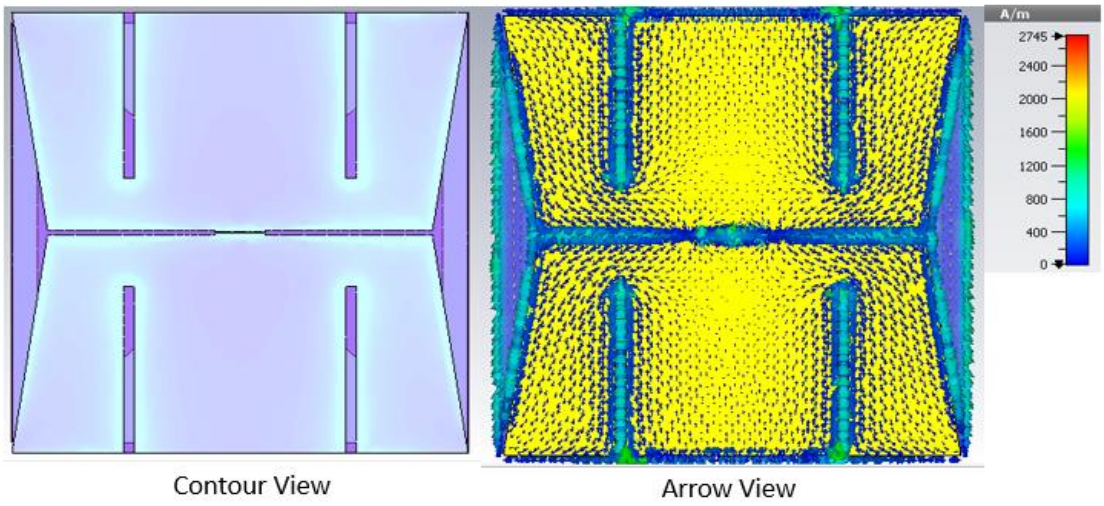

Figure 4. 16: The surface current distribution for top patch (Arrow View on Left, Contour View on Right)

Figure below shows the surface current distribution for middle patch.

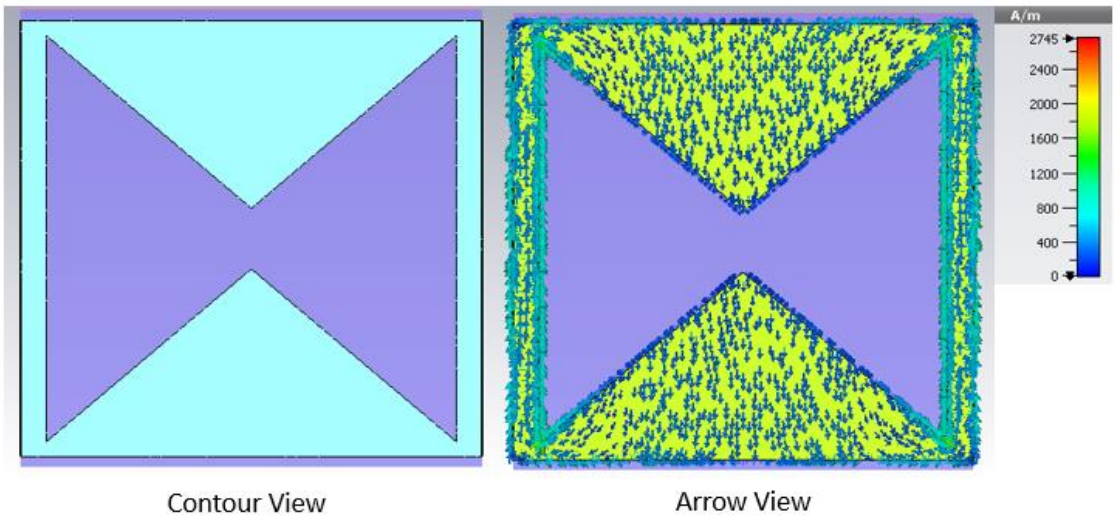

Figure 4. 17: The surface current distribution for middle patch (Arrow View on Left, Contour View on Right)

4.2 Measured Results of the RFID Tag Antenna

All of the measured results are measured by using Voyantic Tagformance measurement system in an anechoic cabinet.

4.2.1 Measured Resonant Frequency, Tag Sensitivity and Realized Gain

The measured resonant frequency of the tag antenna is 0.910 GHz. The measured realize gain of the tag antenna is 1.845 dB. The measured tag sensitivity is -19.645 dBm. Figure below shows the measured realize again and tag sensitivity of the tag antenna.

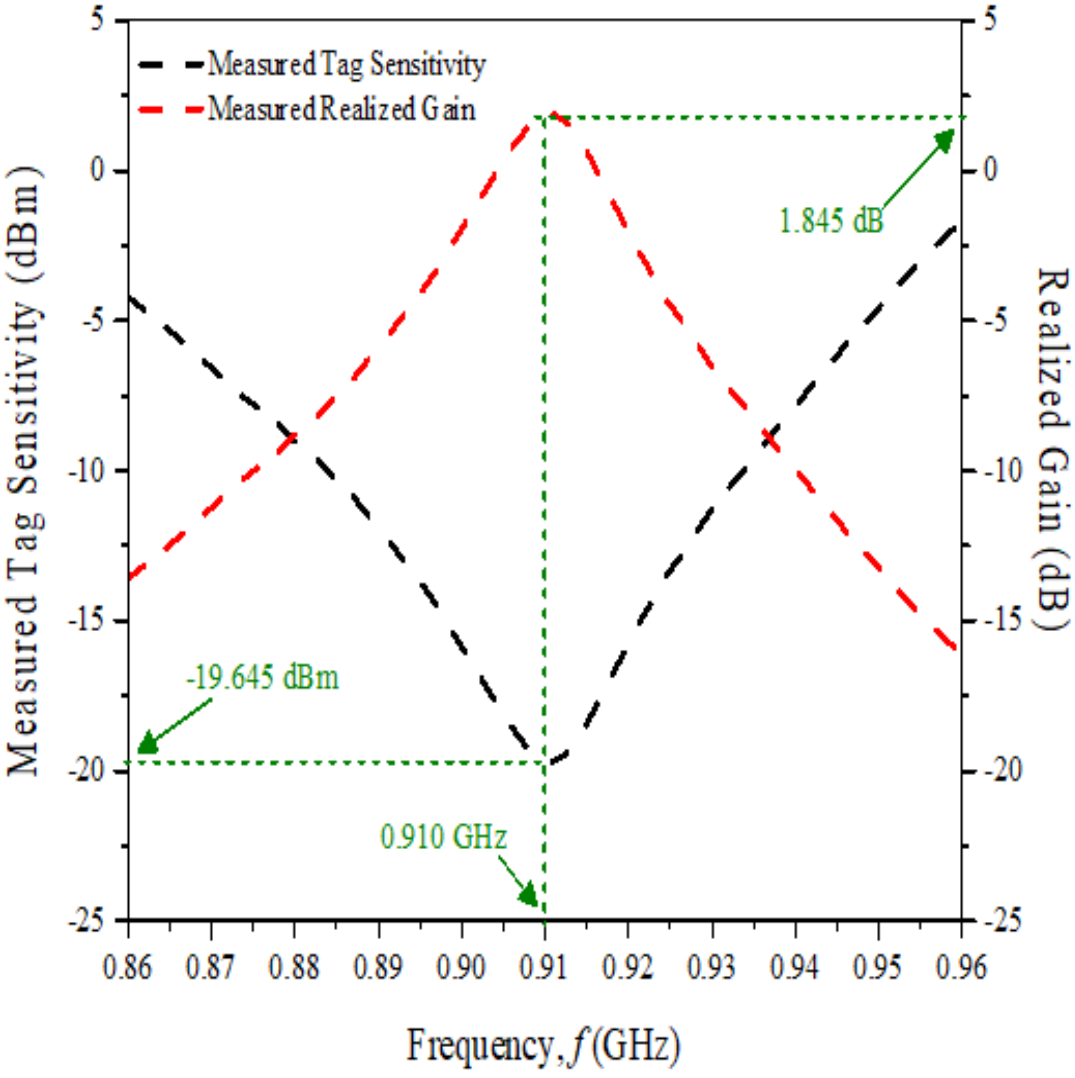

Figure 4. 18: Measured realize again and measured tag sensitivity.

4.2.2 Measured Input Impedance

The measured real input impedance for the antenna is 7.02 Ω while the imaginary input impedance is j180.13 Ω. The total input impedance (real + imaginary) is 7.02 Ω + j180.13 Ω. The figure below shows the measured input impedance of the tag antenna.

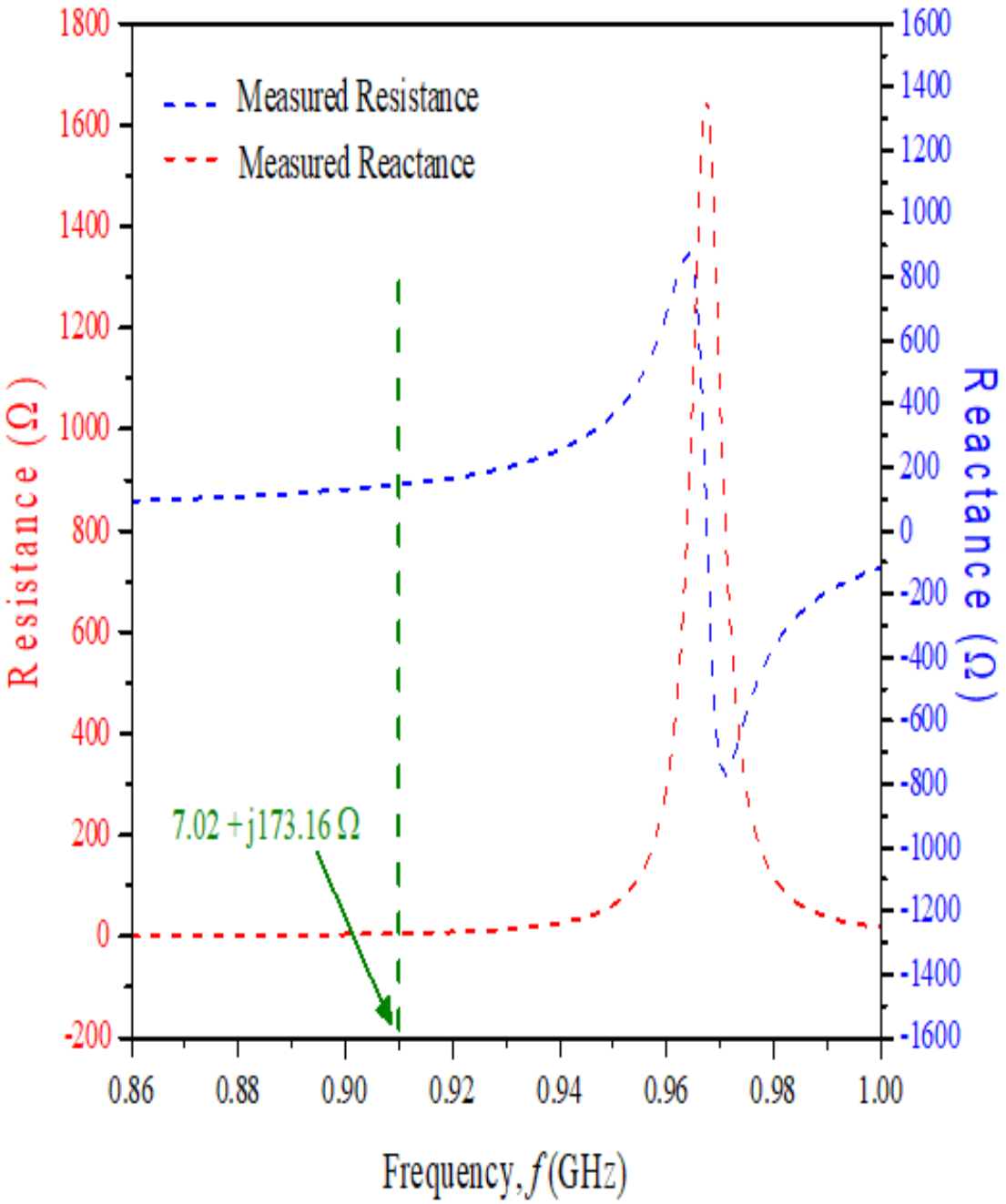

Figure 4. 19: Measured input impedance of the tag antenna.

4.2.3 Measured Read Distance

The antenna's read distance is measured in three different orientations which are x-z plane, y-z plane and x-y plane at 0.910 GHz. The measured read distance of the antenna in x-z plane is 14 m and the read distance in y-z plane is 15 m. The read distance of the antenna in x-y plane is 13 m. Figures below show the measured read distance of the tag antenna in the x-z and y-z and x-y plane.

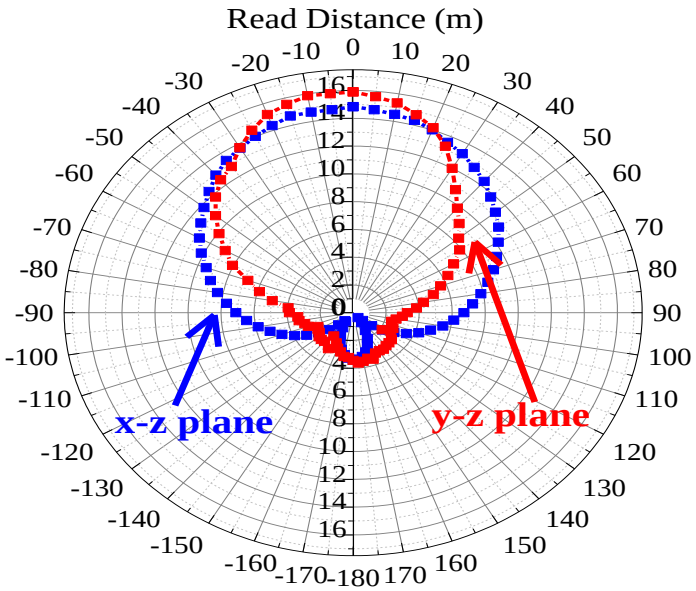

Figure 4. 20: Measured read distance in the x-z and y-z plane.

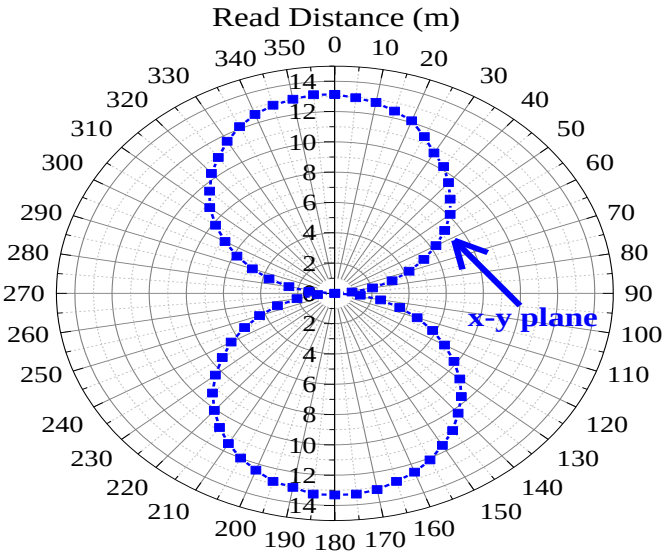

Figure 4. 21: Measured read distance in the x-y plane.

4.2.4 Effect of the Tag Antenna on Different Size of Backing Metal Plate

For all of the above results, the tag antenna is attached onto the metal plate with a size of L x W = (20 cm x 20 cm).

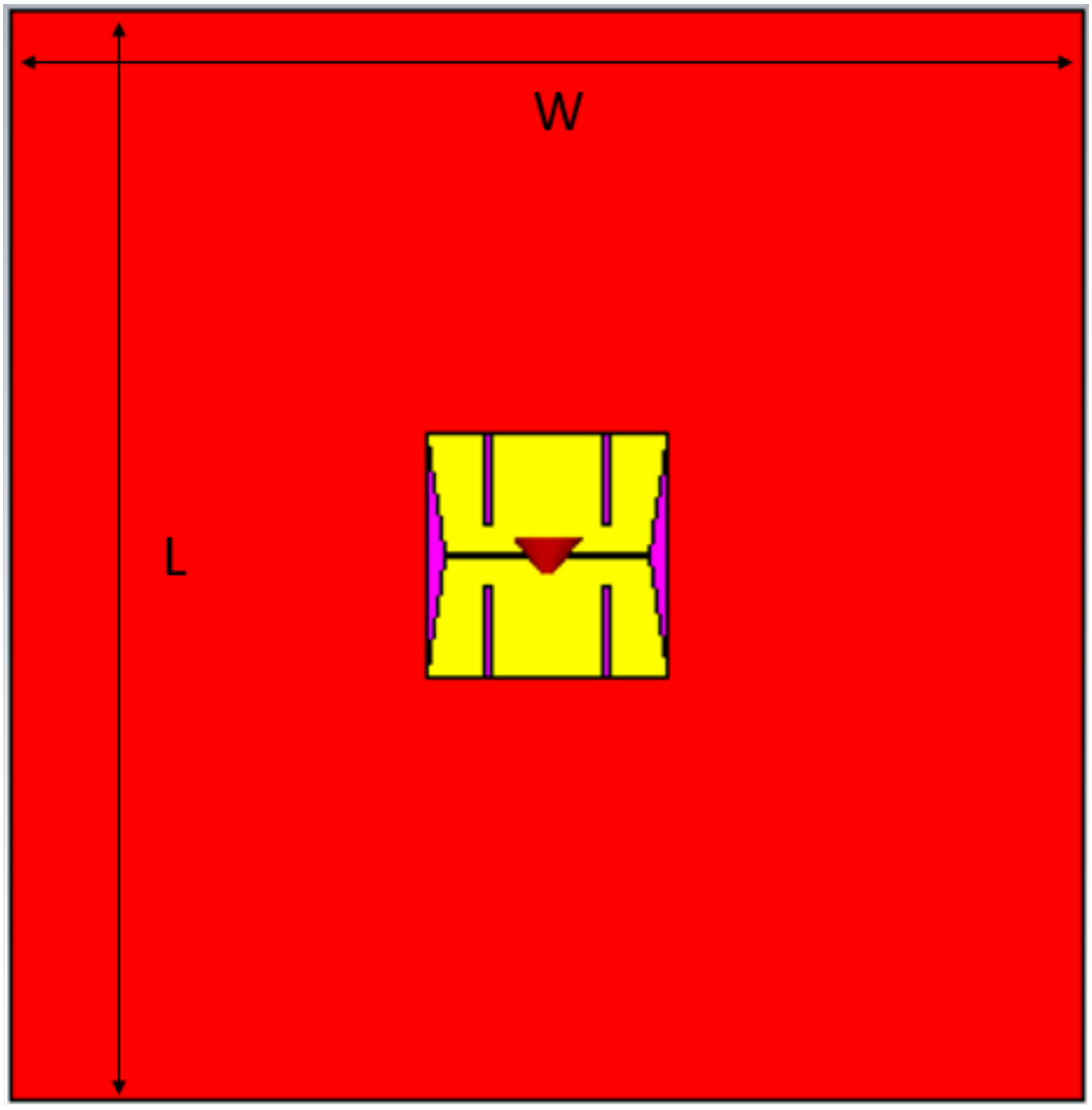

Figure 4. 22: Antenna attached on the backing metal.

In order to verify that the tag antenna can works well in different condition, we try to measure the tag antenna on different sizes of backing metal. Firstly, we vary the length, *L* of the backing metal from 8 cm to 24 cm, while keeping the width, *W* of the backing metal constant. Then, we vary the width, *W* of the backing metal from 8cm to 24 cm, while keeping the length, *L* of the backing metal constant.

Figure below shows the behaviours of the tag antenna by varying the length, *L* of the backing metal. The results show that the resonant frequencies of the tag antenna on different sizes of backing metal are almost the same. This phenomenon shows that the tag antenna can works well in different condition.

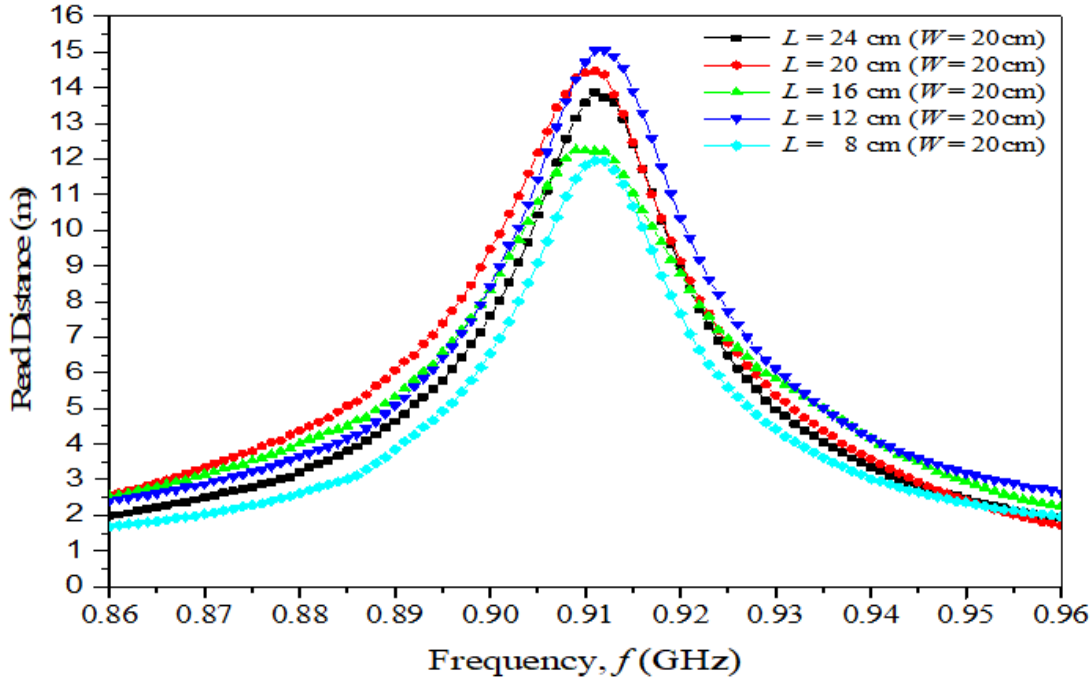

Figure 4. 23: Behaviours of the tag antenna by varying the length, *L*.

Figure below shows behaviours of the tag antenna by varying the width, *W* of the backing metal.

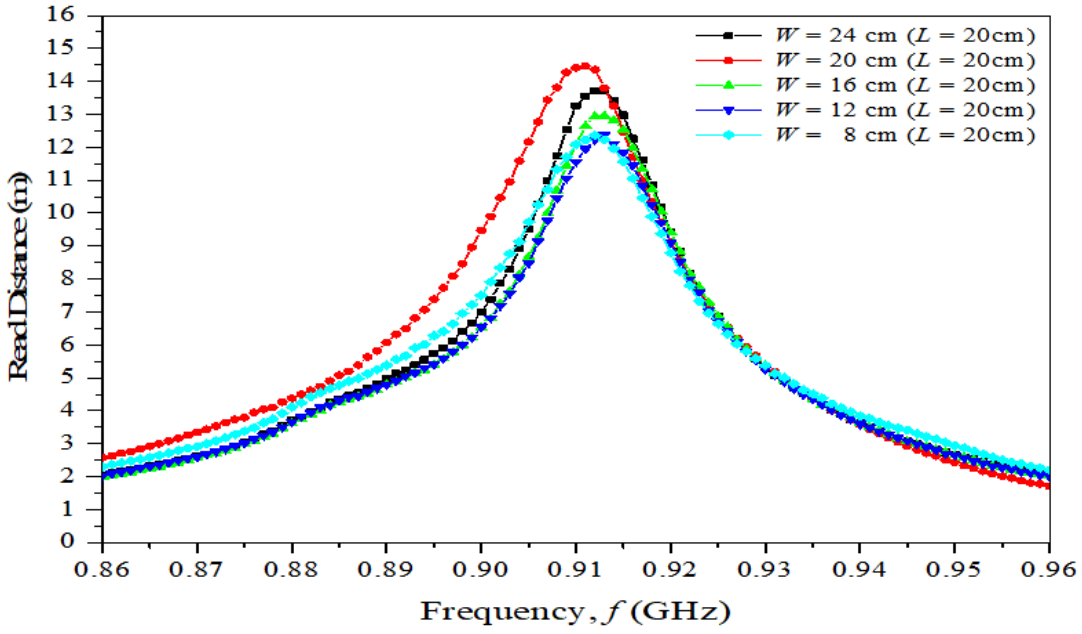

Figure 4. 24: Behaviours of the tag antenna by varying the width, *W*.

4.2.5 Tag Antenna attached on different Household Product.

To further ensure the tag antenna can work perfectly in different situations, the tag antenna is also tested on different household product such as container of biscuit and etc. Figure below show the tag antenna attached on different household product with different dimension.

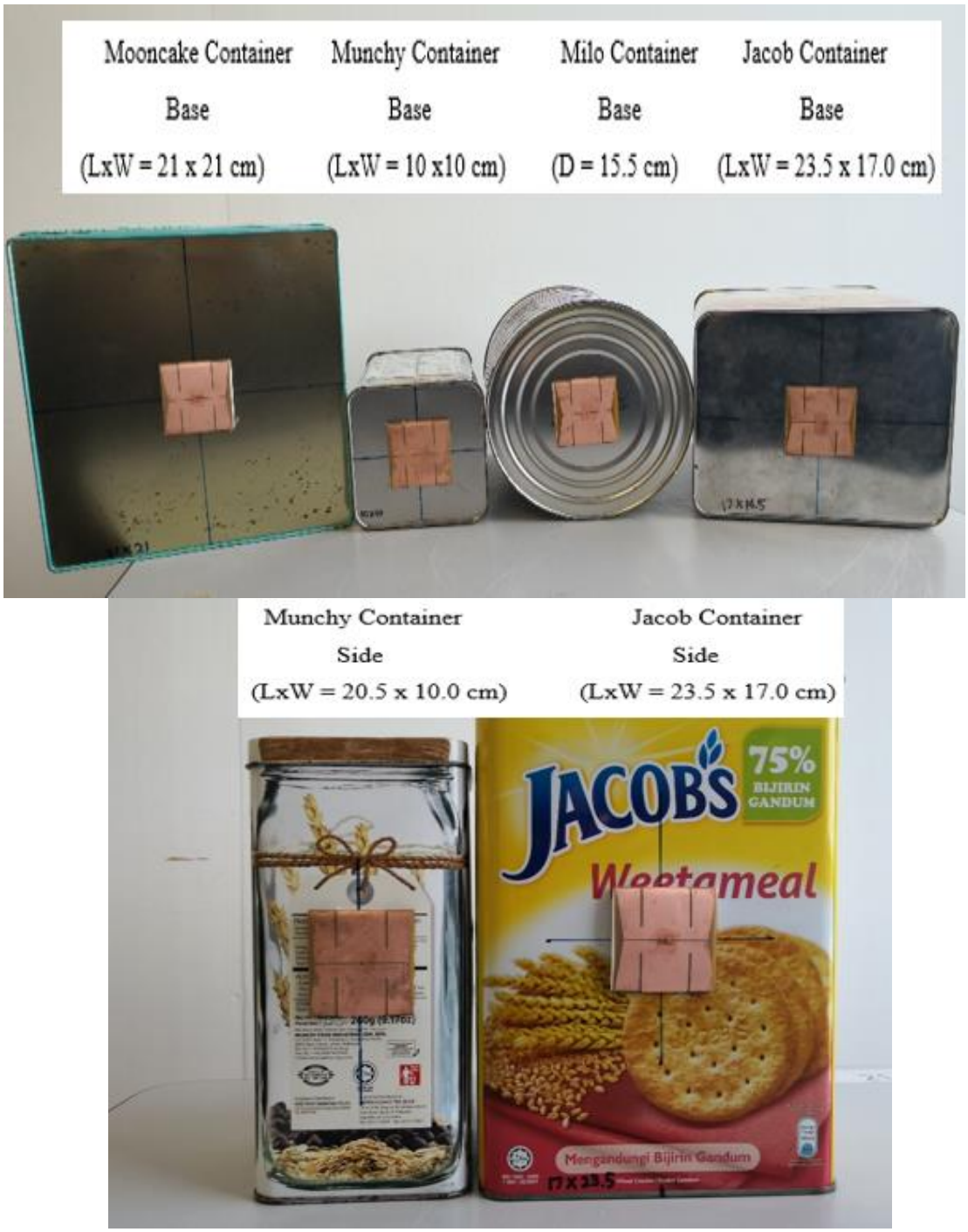

Figure 4. 25: Tag antenna being tested for different dimension of household product.

Graph below shows the behaviour of the tag antenna being attached on different products. From the figure below, it shows that the resonant frequencies of the antenna still looks the same. Besides that, the read distances of the tag antenna also do not vary much. Hence, we can conclude that the tag antenna can work perfectly in different situations.

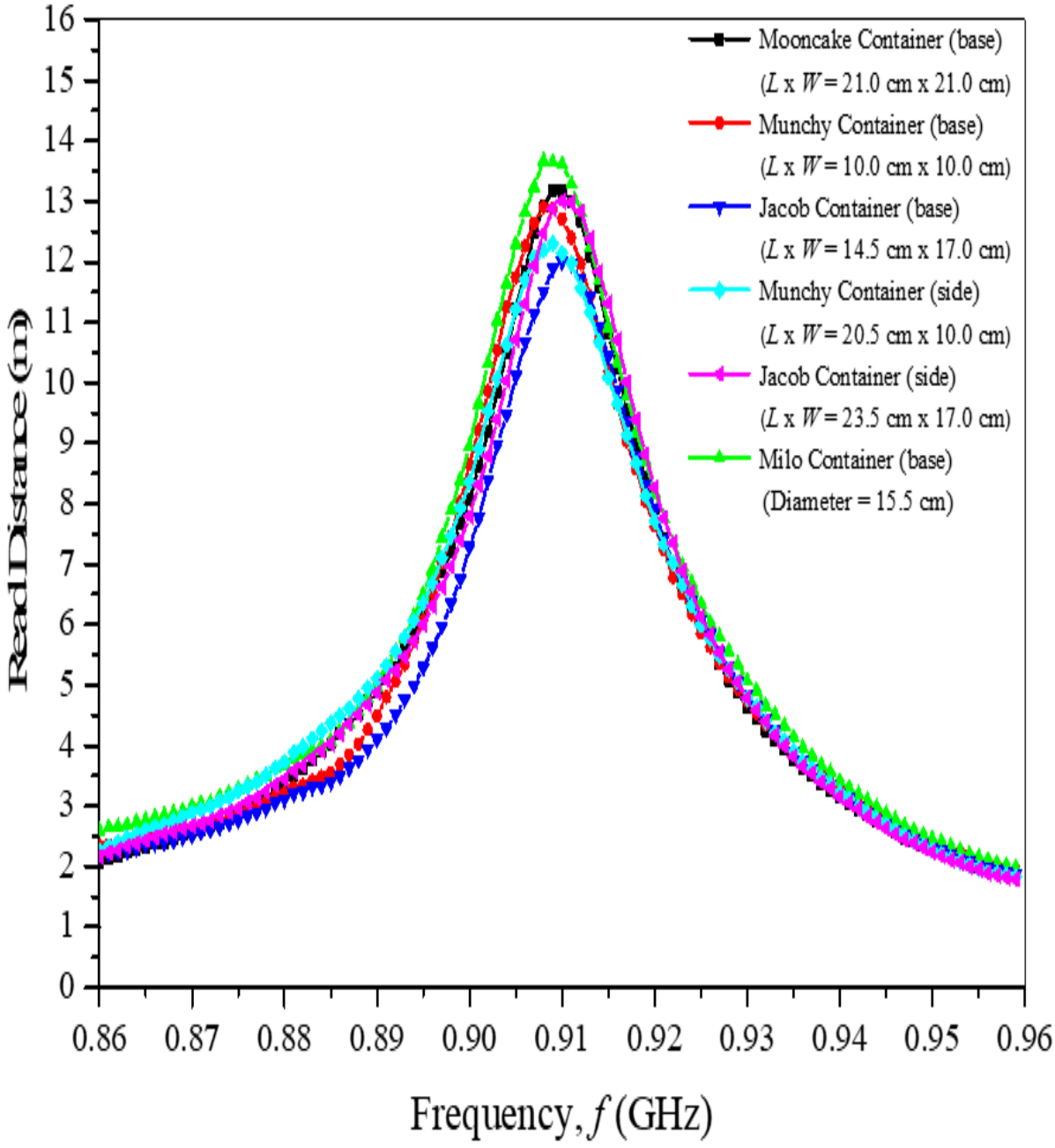

Figure 4. 26: Behaviour of the tag antenna being attached on different household product.

4.3 Comparing Simulated Results and Measured Results

In order to make sure the tag antenna is suitable for mass production, simulated results and measured results must be compared.

4.3.1 Compared Realized Gain and Resonance Frequency

From the collected results, the simulated resonant frequency for the tag antenna is 0.916 GHz while the measured resonant frequency is 0.910 GHz. The difference of resonant frequency is only 0.006 GHz and the percentage error is only 0.0066 %. Besides that, the simulated gain is 2.554 dB while the measured gain is 1.845 dB. Hence, we can conclude that the actual tag antenna can work perfectly since the simulated results and the measure results are not much different. Figure below shows the difference of the resonant frequency and gain between the simulated results and measured results.

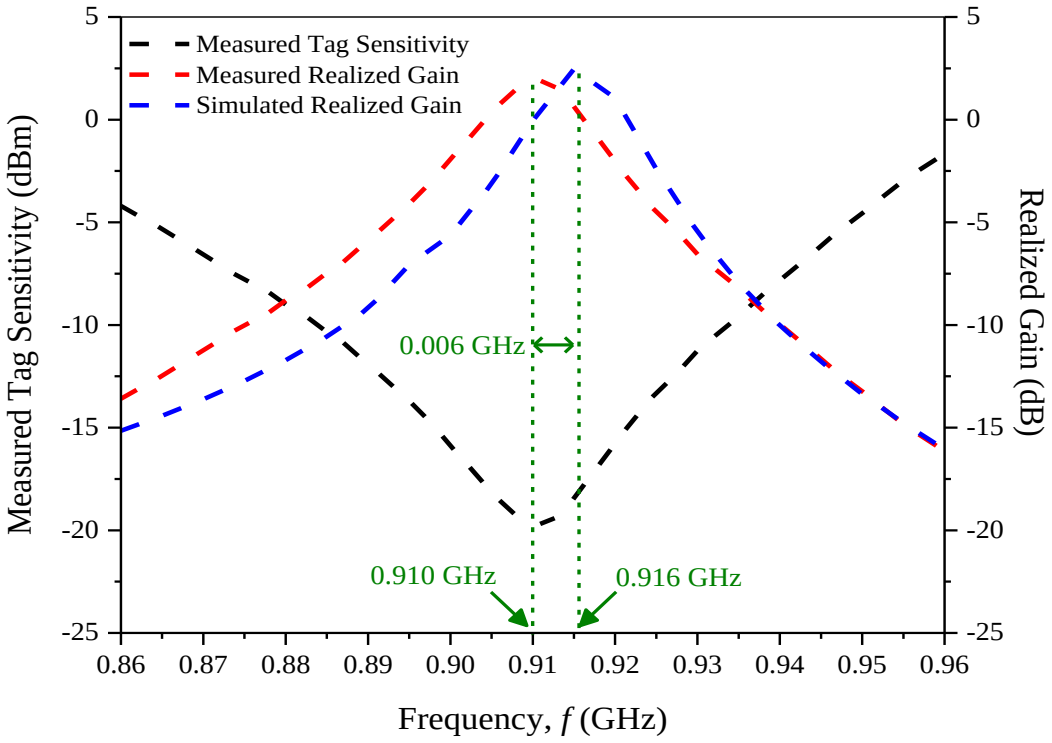

Figure 4. 27: Resonant frequency and gain of simulated results and measured results.

4.3.2 Compared Input Impedance

From the collected results, the simulated input impedance is 7.77 + j162.39 Ω while the measured input impedance is 7.02 Ω + j180.13 Ω. There is not much difference between the simulated input impedance and the measured input impedance. Besides that, figure 4.28 also shows that the simulated input impedance and measured input impedance are almost the same. Hence, we can conclude that the conjugate match is achieved between tag antenna the Monza 5 chip. Figure below shows the comparison between simulated input impedance and the measured input impedance.

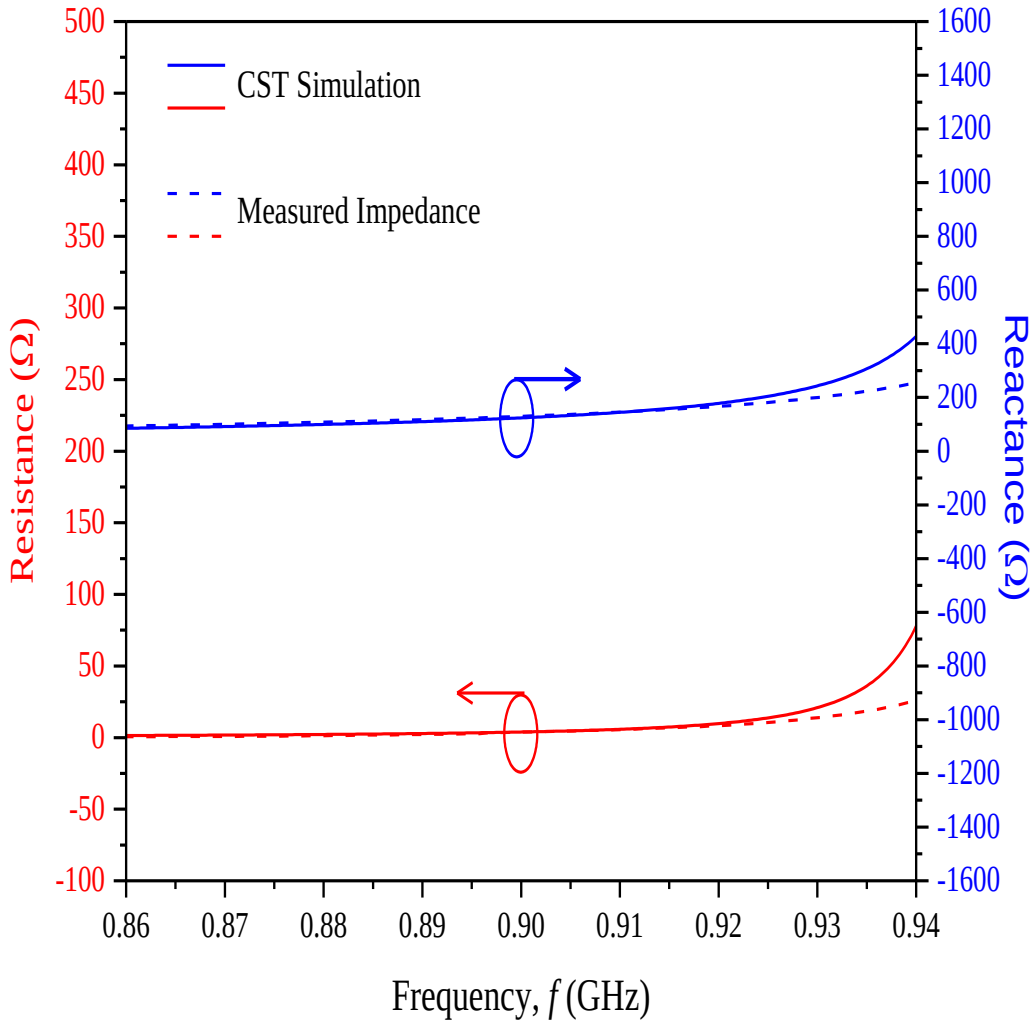

Figure 4. 28: Comparison between simulated input impedance and the measured input impedance.

4.3.3 Summary for Comparison between the Simulation Results and Measured Results.

	Simulation Results	Measured Results
Resonant Frequency	0.916 GHz	0.910 GHz
Input Impedance	7.77 + j162.39 Ω	7.02 Ω + j180.13 Ω
Read Range	12 m	13 m
Realized Gain	2.554 dB	1.845 dB

Table 4. 1: Summary for Comparison between the Simulation Results and Measured Results.

4.4 The Achievement of the Designed Tag Antenna

Table below shows the whether the designed tag antenna meet the pre requirements.

Parameters	Pre-requirements	Achieved
Gain	≤ -3 dB	✓
Resonant Frequency	Between 0.86 GHz to 0.96 GHz	✓
Power Transmission Coefficient	≥ 0.7	✓
Read Distance	≥ 10 m	✓
Microchip Used	Monza 5	✓

Table 4. 2: Table of whether the designed tag antenna meet the pre requirements.

CHAPTER 5

CONCLUSIONS AND RECOMMENDATIONS

5.1 Conclusions

In conclusion, all the objectives are achieved. The designed RFID tag antenna with a simulated resonant frequency of 0.916 GHz and measured resonant frequency of 0.910 GHz can be used within the UHF RFID band from 0.86 GHz to 0.96 GHz. The read distance of the tag antenna is able to reach a considerably long distance of 13 m. Its application will allow object to be tracked by the RFID reader at far distance. All the properties such as realized gain, read distance, parametric analysis and etc of the antenna are studied in detail. The tag antenna can also work perfectly in different situations and environments. This is important since the tag antenna must be able to overcome different signal distortion caused by different environment. Last but not least, the designed RFID tag antenna had matched all the pre-requirements of the project by having a great realized gain, read distance and power transmission.

5.2 Recommendations for future work

A few recommendations needed are made here to enhance the project in the future. Firstly, the bandwidth of the tag antenna can be further broaden so that the tag antenna has larger bandwidth selection. Secondly, the tag antenna can be modified to work at all the regions in the world.

REFERENCES

Abdelaziz, A., 2006. Bandwidth enhansment of microstrip antenna. *Progress In Electromagnetics Research, 63*, pp.311-317.

Chen, Z.N., Qing, X. and Chung, H.L., 2009. A universal UHF RFID reader antenna. *IEEE Transactions on Microwave Theory and Techniques, 57*(5), pp.1275-1282.

Egashira, S. and Nishiyama, E., 1996. Stacked microstrip antenna with wide bandwidth and high gain. *IEEE Transactions on Antennas and Propagation*, *44*(11), pp.1533-1534.

Harrington, R.F., 1960. Effect of antenna size on gain, bandwidth, and efficiency. *J. Res. Nat. Bur. Stand*, *64*(1), pp.1-12.

Huang, C.Y. and Hsia, W.C., 2005. Planar elliptical antenna for ultra-wideband communications. *Electronics Letters*, *41*(6), pp.296-297.

Huang, Y. and Boyle, K., 2008. *Antennas: from theory to practice*. John Wiley & Sons.

IDTechEx, Das, R., & Harrop, P. (2011). *RFID forecasts, players and opportunities 2011-2021*. IDTechEx.

Jackson, D. and Alexopoulos, N., 1985. Gain enhancement methods for printed circuit antennas. *IEEE transactions on antennas and propagation*, *33*(9), pp.976-987.

Liu, X., Liu, Y. and Tentzeris, M.M., 2015. A novel circularly polarized antenna with coin-shaped patches and a ring-shaped strip for worldwide UHF RFID applications. *IEEE Antennas and Wireless Propagation Letters*, *14*, pp.707-710.

Niew, Y. H., Lee, K. Y., Lim, E. H., Bong, F. L., & Chung, B. K. (2019). Patch-loaded Semicircular Dipolar Antenna for Metal-Mountable UHF RFID Tag Design. IEEE Transactions on Antennas and Propagation

Pozar, D.M., 1992. Microstrip antennas. *Proceedings of the IEEE, 80*(1), pp.79-91.

Pues, H.F. and Van De Capelle, A.R., 1989. An impedance-matching technique for increasing the bandwidth of microstrip antennas. *IEEE transactions on antennas and propagation*, *37*(11), pp.1345-1354.

Qian, Y., Sievenpiper, D., Radisic, V., Yablonovitch, E. and Itoh, T., 1998, August. A novel approach for gain and bandwidth enhancement of patch antennas. In *Radio and Wireless Conference, 1998. RAWCON 98. 1998 IEEE* (pp. 221-224). IEEE.

Qiang Cheng, Xiao Yang Zhou, Bin Zhou, Hong Sheng Xu and Tie Jun Cui (2008). A superstrate for microstrip patch antennas. *2008 International Workshop on Metamaterials.*

Rao, K. S., Nikitin, P. V., & Lam, S. F. (2005). Antenna design for UHF RFID tags: A review and a practical application. *IEEE Transactions on antennas and propagation*, *53*(12), 3870-3876.

Sangaran, P. and Margon, K., 2016. *Antenna having a reflector for improved efficiency, gain, and directivity*. U.S. Patent Application 14/860,682.

Sussman-Fort, S.E. and Rudish, R.M., 2009. Non-Foster impedance matching of electrically-small antennas. *IEEE Transactions on Antennas and Propagation*, *57*(8), pp.2230-2241.

Sze, J.Y. and Wong, K.L., 2000. Slotted rectangular microstrip antenna for bandwidth enhancement. *IEEE transactions on antennas and propagation*, *48*(8), pp.1149-1152.

Trembly, B.S., 1985. The effects of driving frequency and antenna length on power deposition within a microwave antenna array used for hyperthermia. *IEEE transactions on biomedical engineering*, (2), pp.152-157.

Yadav, V.S., Sahu, D.K., Singh, Y. and Dhubkarya, D.C., 2010, March. The effect of frequency and temperature on dielectric properties of pure poly vinylidene fluoride (PVDF) thin films. In *Proceedings of the international multiconference of engineers and computer scientists* (Vol. 3, pp. 17-19).

Yang, H. and Alexopoulos, N.I.C.O.L.A.O.S.G., 1987. Gain enhancement methods for printed circuit antennas through multiple superstrates. *IEEE Transactions on Antennas and Propagation*, *35*(7), pp.860-863.